

**LANDSLIDE INVESTIGATION USING ELECTRICAL RESISTIVITY
TOMOGRAPHY (ERT), GEOTECHNICAL TECHNIQUES AND GIS
MAPPING OF SARBALA LANDSLIDE, HATTIAN BALA, AZAD
JAMMU & KASHMIR.**



By

Jawad Niaz

M.Phil. Geology

2021-2023

Department of Earth Sciences

Quaid-i-Azam University, Islamabad, Pakistan

CERTIFICATE

It is certified that **Mr. Jawad Niaz S/O Niaz Ahmed Khan (Registration No. 02112111021)** carried out the work contained in this dissertation under my supervision and accepted in its present form by Department of Earth Sciences as satisfying the requirements for the award of **M.Phil Degree in Geology**.

RECOMMENDED BY

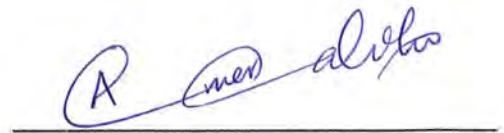
Dr. Aamir Ali
Associate Professor/Supervisor



Dr. Farhan Javed
External Examiner



Dr. Aamir Ali
Chairperson



DEPARTMENT OF EARTH SCIENCES
QUAID-I-AZAM UNIVERSITY
ISLAMABAD

Acknowledgements

This dissertation would not have been possible without the support of many people. First, I would like to express my profound gratitude to my supervisor, Dr. Aamir Ali, for giving me an opportunity to work under his kind supervision. His continuous support, motivation, inspiration, and constructive feedback throughout this research work kept my confidence high. I am very indebted to him for his critical review of the thesis documentation.

I am profoundly grateful to Dr. Aamir Ali, Chairman Department of Earth Sciences Quaid-i-Azam University, Islamabad for his guidance, kind support and especially, facilitating in field survey.

I owe special gratitude to Dr. Abrar Niaz, Assistant professor, Azad Jammu Kashmir for providing technical support for ERT data acquisition. I acknowledge his support in field surveys and data processing.

I greatly appreciate Fahad Hameed, Assistant Professor, university of Azad Jammu and Kashmir for his help in ERT field survey.

I would like to express heartfelt gratitude to my parents for their affection, support, and encouragement throughout my life, without whom I may have not achieve this goal.

Jawad Niaz

ABSTRACT

Landslides are disastrous phenomena causing widespread destruction to landscape, infrastructure, and life throughout the world and mostly in mountainous terrain. The investigated mass movement Sarbala Landslide is located in district Hattian Bala Azad Jammu & Kashmir that was first activated in April 2018 after prolonged rainfalls. This mass movement caused extensive damage to the infrastructure and landscape of the area and still poses a threat to adjoining settlements. This study aims to investigate the slope failure mechanism of Sarbala Landslide using integrated geophysical and Geotechnical techniques.

To characterize the Sarbala Landslide, techniques including geological field work, electrical resistivity tomography (ERT), geotechnical techniques, and GIS mapping were applied to evaluate the surface and subsurface dynamics of the Sarbala Landslide. Multiple field surveys were conducted in which soil samples were collected and six ERT profiles using the Wenner-Schlumberger array were acquired in different parts of the Sarbala Landslide. ERT results reveal that the sliding mass of the Sarbala landslide mainly comprises saturated colluvium and debris that causes low resistivity in tomograms. Saturation of slope forming material is a major cause contributing to instability of Sarbala Landslide. A well-developed Slip surface is observed between unconsolidated landslide mass and underlying bedrock based upon resistivity contrast.

The Atterberg limits of the landslide material indicated low to medium plastic behavior of Sarbala landslide. According to the study, soil is mostly sand with minor silt and clays and have high porosity and permeability, therefore more water entered the subsurface and decreases strength by increasing pore water pressure, causing the soil to break down and resulting in slope failure.

In addition, tectonically this area is active and bounded by two active faults i.e., are Bagh Balakot fault and Jhelum fault. Distance to fault map reveals that these two faults are located within the diameter of 3-10 km from Sarbala landslide and play key role for the triggering of landslide. Well-developed scarps and large-scale tensional cracks in landslide depict the active nature of landslide. This study indicates that Sarbala Landslide is an active mass movement. Besides active tectonics of the study area, hydrogeology of the slope forming mass is a major factor reducing the stability of Sarbala Landslide. This study suggests the implication of more advanced research for monitoring of Sarbala landslide in future.

Table of Contents

1 INTRODUCTION	1
1.1 Background.....	1
1.2 Tectonic Setting.....	3
1.2.1 Hazara Kashmir syntaxis.....	5
1.3 Stratigraphy of the Study Area	6
1.3.1 Murree Formation.....	6
2 LITERATURE REVIEW	8
2.1 Previous work.....	8
2.2 Use of Geophysical Techniques for Landslide Investigation	9
2.3 Use of Geotechnical Techniques for Landslide Investigation	10
3 LANDSLIDE TYPES AND CAUSES.....	11
3.1 Morphology of Landslide.....	11
3.1.1 Crown.....	11
3.1.2 Main scarp.....	12
3.1.3 Head	12
3.1.4 Main body	12
3.1.5 Toe	12
3.1.6 Slip Surface or Surface of Rupture	12
3.1.7 Flanks.....	12
3.2 Types of Landslides	12
3.2.1 Falls.....	13
3.2.2 Topples.....	14
3.2.3 Slides.....	14
3.2.4 Lateral Spreads.....	15
3.2.5 Flows.....	16
3.2.6 Debris Flow.....	16
3.2.7 Debris Avalanche.....	16
3.2.8 Earth Flow.....	16
3.2.9 Creep.....	16
3.2.10 Complex Slide.....	17

3.3 Factor Causing Landslide.....	17
3.3.1 Triggering Factors of Landslide.....	17
3.3.2 Geological Conditions.....	18
2.3.3 Topographical Conditions.....	18
2.3.4 Hydrological Conditions.....	19
2.3.5 Structural Conditions.....	19
4 METHODOLOGY AND RESOURCES.....	20
4.1 Electrical Resistivity Tomography.....	21
4.2 Relationship between Resistivity and Geology.....	22
4.3 Data Acquisition and Processing.....	23
4.3.1 Instrumentation	23
4.3.2 Electrode Configuration.....	24
4.4 Geotechnical Approaches.....	25
4.4.1 Laboratory Soil Testing.....	25
4.4.2 Soil Test.....	25
4.4.3 Sieve Analyses	26
4.4.4.1 Liquid Limit.....	27
4.4.4.2 Plastic limit	27
4.4.4.3 Plasticity Index.....	28
4.5 Liquid Limit by Casagrande method.....	28
4.5.1 Apparatus	28
4.5.2 Procedure.....	29
4.6 Plastic Limit Procedure.....	29
4.7 Specific Gravity.....	29
4.7.1 Apparatus.....	29
4.7.2 Procedure	29
4.8 Proctor Compaction Test.....	30
4.8.1 Apparatus.....	30
4.8.2 Procedure	30
5 RESULTS	31
5.1 Landslide Characteristics.....	31
5.1.2.1 Main Scarp	31

5.1.2.2 Cracks.....	32
5.1.2.3 Depletion Zone.....	33
5.1.2.4 Transition Zone.....	33
5.1.2.5 Deposition Zone	33
5.1.2.6 Type of Movement in Sarbala Landslide.....	35
5.2 ERT Results.....	36
5.2.1 ERT 01 Section.....	36
5.2.2 ERT 02 Section.....	37
5.2.3 ERT 03 Section.....	39
5.2.4 ERT 04 Section.....	40
5.2.5 ERT 05 Section	42
5.2.6 ERT 06 Section.....	44
5.3 Electrical Resistivity 3D Models.....	45
5.4 Geotechnical Results.....	47
5.4.1 Sieve Analysis.....	47
5.4.2 Specific Gravity.....	48
5.4.3 Atterberg Limit.....	49
5.4.3.1 Liquid Limit of Right Flank.....	49
5.4.3.2 Liquid Limit Centre of Landslide.....	50
5.4.3.3 Liquid Limit of Left Flank.....	50
5.5.4.1 Proctor Compaction Test of Right Flank.....	51
5.5.4.2 Proctor Compaction Test of Left Flank.....	52
5.5.4.3 Proctor Compaction Test Centre of Landslide.....	52
6 DISCUSSION AND CONCLUSIONS	53
6.1 Discussion	53
6.2 Conclusions.....	56
6.3 Recommendations	56
7 REFERENCES.....	58

LIST OF Figures

Fig. 1.1 (a) Location map of the study area, Landslide extend shown with red polygon. 1.1(b) the location of study area on map of Azad Kashmir. 1.1 (c) shows the location of the study area with red rectangle.	2
Fig. 1.2 Regional tectonic map of the northwest Himalayas in Pakistan (Basharat et al., 2012; Avouac et al., 2006; Greco, 1991; Baig and Lawrence, 1987; Calkins et al., 1975; Wadia,1931).....	4
Fig. 1.3 Geological and structural map of HKS after (Wadia, 1928) and (Khan & Ali,1994)...	7
Fig. 3.1 Cross sectional diagram of a landslide illustrating landslide geometry. (Varnes, 1978).....	11
Fig. 3.2 Schematic diagram showing the types of landslides as classified by Varnes(1978)...	13
Fig. 4.1 Schematic flow chart of the research methodology.....	20
Fig. 4.2 ERT Survey procedure and current flow pattern.....	22
Fig. 4.3 Resistivity of different rock.....	23
Fig. 4.4 Terameter SAS 4000 (Sweden) ABEM instrument with its accessories.....	24
Fig.4.5 Different mesh sizes are arranged on shaker for gradation of soil sample.....	27
Fig 4.6 Apparatus for liquid limit by Casagrande method.....	28
Fig.5.1 Massive land deformation and tilting of trees caused by Sarbala Landslide.....	31
Fig.5.2a. Main scarp of landslide., b - Main scarp at the head of the landslide near road C- Fractured sandstone of the Murree Formation exposed at mainscarp.....	32
Fig.5.3a&b - Slippage of a block of soil due to cracks at crown.....	33
Fig. 5.4 Map showing the zones of Sarbala landslide.....	34
Fig. 5.5 Geological map of Sarbala landslide.....	34

Fig. 5.6 Downslope view of rotational earth slide documented in Sarbala Landslide.....	35
Fig. 5.7 showing translational slide in Sarbala landslide.....	35
Fig. 5.8 Google earth imagery showing ERT profile 1. This ERT profile was taken from near the crown of Sarbala Landslide.....	36
Fig. 5.9 Displays distribution of resistivity values in ERT section 1 taken from near the crown of Sarbala Landslide. Black dashed line shows the slip surface of landslide. Color rectangles showing the resistivity values.....	37
Fig. 5.10 Google earth imagery showing ERT Profile 2. This ERT profile was collected from road that is damaged by Sarbala Landslide.....	38
Fig. 5.11 Displays distribution of resistivity values in ERT section 2. This ERT profile was taken from road that is damaged by Sarbala Landslide. Black dashed line shows the slip surface of landslide. Color rectangles showing the resistivity values.....	39
Fig. 5.12 Google earth imagery showing ERT Profile 3. This ERT profile was taken from below the road.....	39
Fig. 5.13 Displays distribution of resistivity values in ERT 3 taken from below the road. Black dashed line shows the slip surface of landslide. Color rectangles showing the resistivity values.....	40
Fig. 5.14 Google earth imagery showing ERT Profile 4. This ERT profile was taken from the center of Sarbala Landslide.....	41
Fig. 5.15 Displays distribution of resistivity values in ERT section 4 taken in Sarbala Landslide. Black dashed line shows the slip surface of landslide. Color rectangles showing the resistivity values.....	42
Fig. 5.16 Google earth imagery showing ERT Profile 5. This ERT profile is taken from near the toe of Sarbala Landslide.....	43

Fig. 5.17 Displays distribution of resistivity values in ERT 05 taken in Sarbala Landslide. Black dashed shows the slip surface of landslide. Color rectangles show the resistivity values.....	44
Fig. 5.18 Google earth imagery showing ERT Profile 6. This ERT profile is taken Vertically from north to south of Sarbala Landslide.....	44
Fig. 5.19 Displays distribution of resistivity values in ERT section6 taken vertically from north to south of Sarbala Landslide. Color rectangles showing the resistivity values.....	45
Fig. 5.20 3D view of ERT profiles in different directions.....	46
Fig. 5.21 3D view of ERT profiles in different directions.....	46
Fig. 5.22 3D view of ERT profiles in different directions.....	46
Fig. 5.23 showing particle distribution curve of samples collected from Sarbala landslide.....	48
Fig.5.24 Soil Classification System by AASTHO.....	49
Fig. 5.25 Liquid limit of Right flank.....	50
Fig. 5.26 Liquid limit Centre of slide.....	50
Fig. 5.27 liquid limit graph of Left flank.....	51
Fig. 5.28 Standard proctor compaction curve showing optimum moisture content and maximum dry density from right flank of landslide.....	51
Fig.5.29 Standard proctor compaction curve showing optimum moisture content and maximum dry density from left flank of landslide.....	52
Fig. 5.30 Standard proctor compaction curve showing optimum moisture content and maximum dry density from center of landslide.....	52
Fig.5.31 Map showing distance to fault in the study area.....	54
Fig.5.32 Historical image after 2005 Kashmir earthquake showing movement at study area before the landslide occurs.....	55

Chapter 1

INTRODUCTION

1.1 BACKGROUND

The landslide is descending movement of material under the action of gravity (Cruden *et al.*, 1996). Many activating mechanisms like extreme precipitation, shaking of the earth and anthropogenic activity can cause a landslide. In mountainous regions such as Pakistan, landslides are the main cause of loss of life, damages to communication links, and financial losses. Landslides may be caused by either natural or man-made activity in the mountainous region of Pakistan. The Himalayan Mountains are among the most dangerous in the world because of weak geological components, uneven character, and seismically very active zones. According to Khan (2006), approximately 30% of the world's elevated slope occurs in Himalayan regions. As a result, landslides are widespread in Pakistan's N-W Himalayas, which is a tectonically active region with uneven terrain. These landslides cause a large loss of human life, the ruin of the road, property, and the scenic beauty of the area (Basharat, 2012). Landslides have become increasingly common in the region because of deforestation (Rieux *et al.*, 2007). The geophysical approaches to determine subsurface data give reliable information about slip surface, lithology, and mass movement of landslide (Perrone *et al.*, 2004).

It is vital to have comprehensive knowledge about the geological and geotechnical aspects to develop efficient solutions for the stability and characteristics of landslides. Geophysical approaches used for landslide investigation may give reliable data about the internal structure of the landslide such as probable slip surface and lithology. Knowledge of the internal structure and mechanical properties of slope forming material is of utmost importance for taking measures of slope stability. Various geophysical methods are being used by the scientific community to investigate slope failure mechanisms, delineate boundaries of material, and assess the mechanical properties of slope forming material. Electrical Resistivity Tomography (ERT), a geoelectrical tool has been largely used to investigate landslide phenomena. Batayneh and Al-Diabat (2002) conducted the ERT survey to investigate the landslide geometry and dynamics of landslides. Hence to analyze the characteristics of the Sarbala landslide Geotechnical and active geophysical technique ERT has been used.

In this research work, the Sarbala landslide is selected for analysis as it is continuously affecting nearby infrastructure and the main road which is the only connection to nearby villages. The study area is in hilly Sub-Himalayan region of Pakistan. The Main Boundary Thrust (MBT) in the north separates

the Sub Himalayas from Lesser Himalayas (Gansser, 1981). The whole region is tectonically distorted because of active Jhelum fault and Main Boundary Thrust (MBT) present in its vicinity. The projected area is situated near Sudhan Gali, District Bagh Azad Jammu and Kashmir which has coordinate 73°43'31.38" to 73°43'22.04" E longitudes and from 34° 5'25.22" to 34° 5'25.11"N latitude. It is bordered by Muzaffarabad district in the north, Poonch district in the south, Rawalpindi, and Abbottabad on the west. It is topographically mountainous throughout district Hattian, usually sloping north-east to south-west. The mountains are particularly dominated by coniferous and pine forests. The study area is located at an altitude of 7000 feet above sea level. The average annual precipitation of the area is 1500 mm. The weather in the area varies from hot to moderate. The weather is pleasant in summer and cold in winter. The Hattian area was severely damaged by October 8, 2005, Kashmir earthquake. The research area location map is shown below (Fig 1.1).

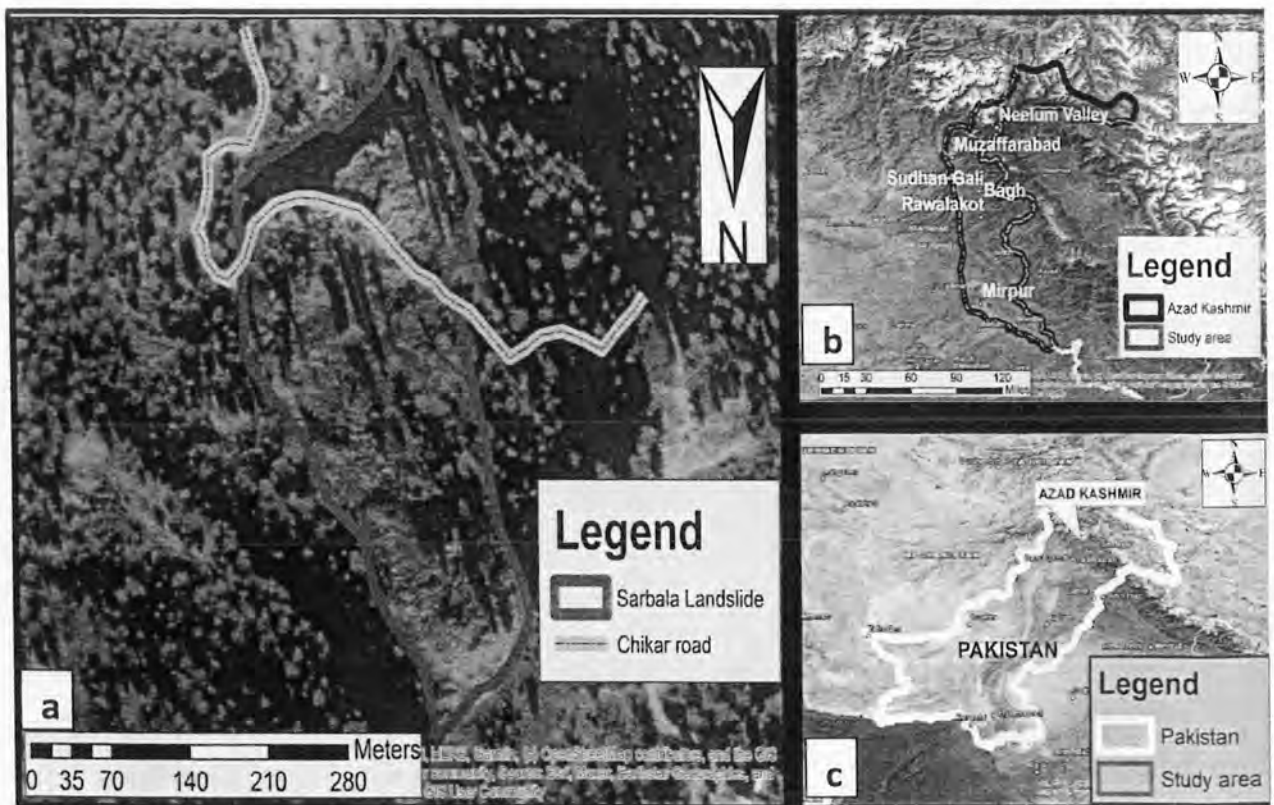


Fig. 1.1 (a) Location map of the study area, landslide extend shown with red polygon. 1.1 (b) the location of study area on map of Azad Kashmir. 1.1 (c) shows the location of the study area with red rectangle.

This research work focuses on Geotechnical investigation of soil and ERT technique by utilizing various electrode configurations to know the subsurface structure of the Sarbala landslide. In Geotechnical different soil tests were performed on the soil sample taken from the landslide body such as grain size distribution, water content and Atterberg limit of the soil. The primary goals of our research are to determine the probable slip surface, lithology, grain size distribution, and moisture content of landslide. Subsurface lithology is also interpreted by using the ERT technique.

1.2 Tectonic Setting

The study site is situated in the northwestern Himalayas of Pakistan which denotes a significant bend in the Himalayan Mountain system known as Western Syntaxis (Wadia, 1931). Tectonically Pakistan lies in the northwestern edge of the Indian Plate. The Himalayas are rising at a rapid rate of $>7\text{mm}$ annually from the last 10 Ma (Kazmi & Jan, 1997). This rapid uplift rate forms one of the highest mountain belts of the world which is nearly 2,500 km long and 160-400 km wide called Himalayan Mountains.

Tectonically, the Himalayan collision zone in eastern Kashmir is separated by Gansser (1964) using lithological, structural, and geomorphological criteria, the Himalayas are divided from south to north by faults, MBT separate the Sub Himalaya from Lesser Himalaya and Main Central Thrust (MCT) separate Higher Himalaya from Lesser Himalayas (Fig 1.2). Main Boundary Thrust (MBT) is a major frontal thrust of the Himalayan Mountain chain which loops around HKS. Main Central Thrust (MCT) separates Lesser Himalayas from Higher Himalayas. Higher Himalayas represent Indian basement rock units and cover rock sequences (Greco, 1989). The Lesser Himalayas lie in the North of MBT and south of MCT. The Lesser Himalayas contain mainly sedimentary and Precambrian to Tertiary-aged metasedimentary rock units (Greco, 1989). The tectonic unit present South of MBT is called the Sub Himalayas which comprises of the northern portion of the Indian Shield which underlies the cover sequence of Tertiary age (Greco, 1989).

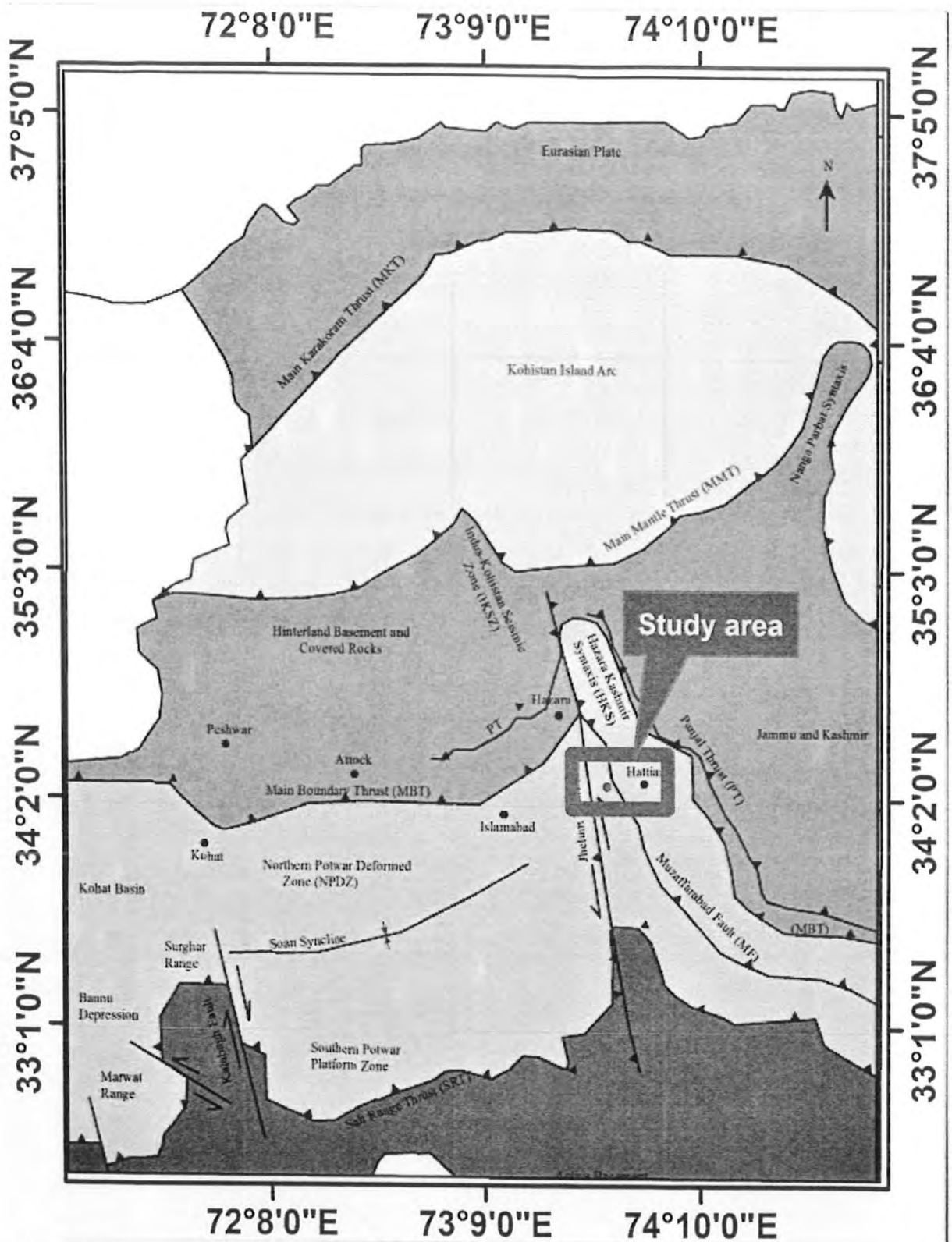


Fig.1.2 Pakistan's northwest Himalayas are depicted on a regional tectonic map. (Avouac et al., 2006; Basharat et al., 2012; Greco, 1991; Wadia, 1931).

The study site Sarbala landslide is in part of Himalayas known as Sub Himalayas. There is another subdivision of the Himalayas by Coward et al., (1988) which divides the Himalayas into an external zone and internal zone (called foreland zone and hinterland zone respectively) based on regional characteristics. The Hinterland zone is bounded by MMT in the South which represents the crystalline rocks of Hazara, Kashmir, Narran, and Swat while the foreland zone which is also called the foreland fold-thrust belt contains sedimentary rock suits of low hill ranges. Panjal Thrust (PT) provides a boundary between hinterland and foreland zones (Baig & Lawrence, 1987). In Kaghan, Hazara, and Azad Kashmir, the Precambrian basement and Paleozoic-Mesozoic cover of the internal zone of the Indian plate are located north of the Panjal Thrust. The exterior zone of the Himalayan collision zone is created by the Paleozoic to Cenozoic folded and imbricated sedimentary sequence that lies between the Panjal Thrust (PT) and the Salt Range Thrust (SRT).

The Tertiary molasse deposits are present in the Sub Himalayas which mainly contain rock units of Eocene and Miocene age. The most significant tectonic elements of Sub-Himalaya are MBT, HFT and JF. HFT is also termed Muzaffarabad Fault (MF) or Bagh Balakot Fault (BBF). It is north-west to the northeast striking fault which extends from Balakot to Bagh and Indian administrated Kashmir through Jhelum River valley (Baig et al., 2010). Muzaffarabad Fault demarcates the boundary between Miocene Murree Formation and Cambrian Abbottabad Formation (Calkins et al., 1975). Jhelum Fault (JF) is an upright strike-slip fault trending north-south that marks the southern continuity of the western limb of Hazara Kashmir Syntaxis (HKS) from Muzaffarabad. From Kohala to Muzaffarabad it extends along River Jhelum. Between Muzaffarabad and Rara (a village located on the junction of Kunhar and Jhelum River). It set a clear boundary between Miocene Murree Formation in the East and Precambrian Hazara Formation. South of Rara village JF marks the contact between Miocene Murree Formation and Mesozoic Rara Formation comprising dolomites, limestones and quartzites (Greco, 1989). Main Boundary Thrust (MBT) is a major frontal thrust of the Himalayan Mountain chain which loops around HKS. Rock units of the Lesser Himalaya (hanging wall) are demarcated by MBT from the molasse deposit of Sub Himalayas (footwall). In HKS, MBT has been offset by Jhelum Fault (Baig & Lawrence, 1987).

1.2.1 Hazara Kashmir Syntaxis

Northern Pakistan also has two major structural bends, the northern bend is called Nanga Parbat Syntaxis (NPS), and the southern bend is termed as Hazara Kashmir Syntaxis (HKS). In the northwest corner of the Himalayas, the HKS tectonic bend is the most prominent. The Indo-Eurasian Plate

Collision has caused sedimentary rocks and metamorphic rock to fold and imbricate around HKS (Bossart et al., 1988; Calkins et al., 1975). In HKS rock units make a hairpin-like bend. This bend on a regional scale was designated as the NW Himalaya Syntaxis by Wadia (1931) and later called as Hazara Kashmir Syntaxis by different authors (Baig & Lawrence, 1987; Greco, 1989). Major structural elements present in HKS are PT, MBT, JF, MF and Muzaffarabad Anticline. At the eastern limb and apex of the HKS, PT distinguishes the Carboniferous-Triassic Panjal Formation from the Precambrian Tanol Formation, whereas at the western limb of the HKS, PT divides the Precambrian Tanol Formation from the Precambrian Hazara Formation. In the core of HKS carbonate units of Cambrian Abbottabad Formation, Paleocene-Eocene sequence of clays, shales, limestones, siltstone, and Miocene molasse deposits of Murree and Kamlial Formation are present (Fig 1.3) (Baig & Snee, 1995; Greco, 1989).

1.3 Stratigraphy of the Study Area

1.3.1 Murree Formation

The Murree Formation denotes the lower Rawalpindi Group (Cheema, 1977; Pinfold, 1918). The name is derived from the Murree hills in the Rawalpindi District. The Murree Formation is composed of a thick fluvial sequence which contains brown to greenish-grey and red sandstone, with minor intraformational conglomerate, dark red and purple clays (Kazmi & Abbasi, 2008; Kazmi & Jan 1997; Shah, 1977). (Wynne, 1874) divided the Murree Formation into upper and lower units. The lower unit is comprised of mainly argillaceous units whereas the upper unit has dominantly arenaceous rocks. Murree formation consists of cyclic deposits of clays, siltstone, and sandstone. Beds of calcareous sandy conglomerate at some places are interposed with the sandstone (Calkins et al., 1975) at the lower part of the formation (Shah, 1977). The formation contains many fining upward cycles of deposition, containing shales, siltstones, and sandstones (Turab, 2012). Siltstone is the major component of the Murree Formation and is comprised of green and red argillaceous silts. The sandstone is green, grey, and red colored, medium to coarse-grained. The sorting in sandstone of the Murree Formation is moderate whereas it is graded bedded and cross bedded at places. The Murree Formation denotes the molasse deposits of the Himalayan orogeny (Mughal et al., 2018).

The exact thickness of the Murree Formation is unknown in the study site due to folding and thrusting. In Azad Kashmir, the thickness of the Murree Formation varies, and in the Muzaffarabad region, it has been measured at 1500 meters. The lower contact of the Murree Formation is with Kuldana Formation and upper contact with Kamliyal Formation is transitional (Munir-ul-Hassan et al.).

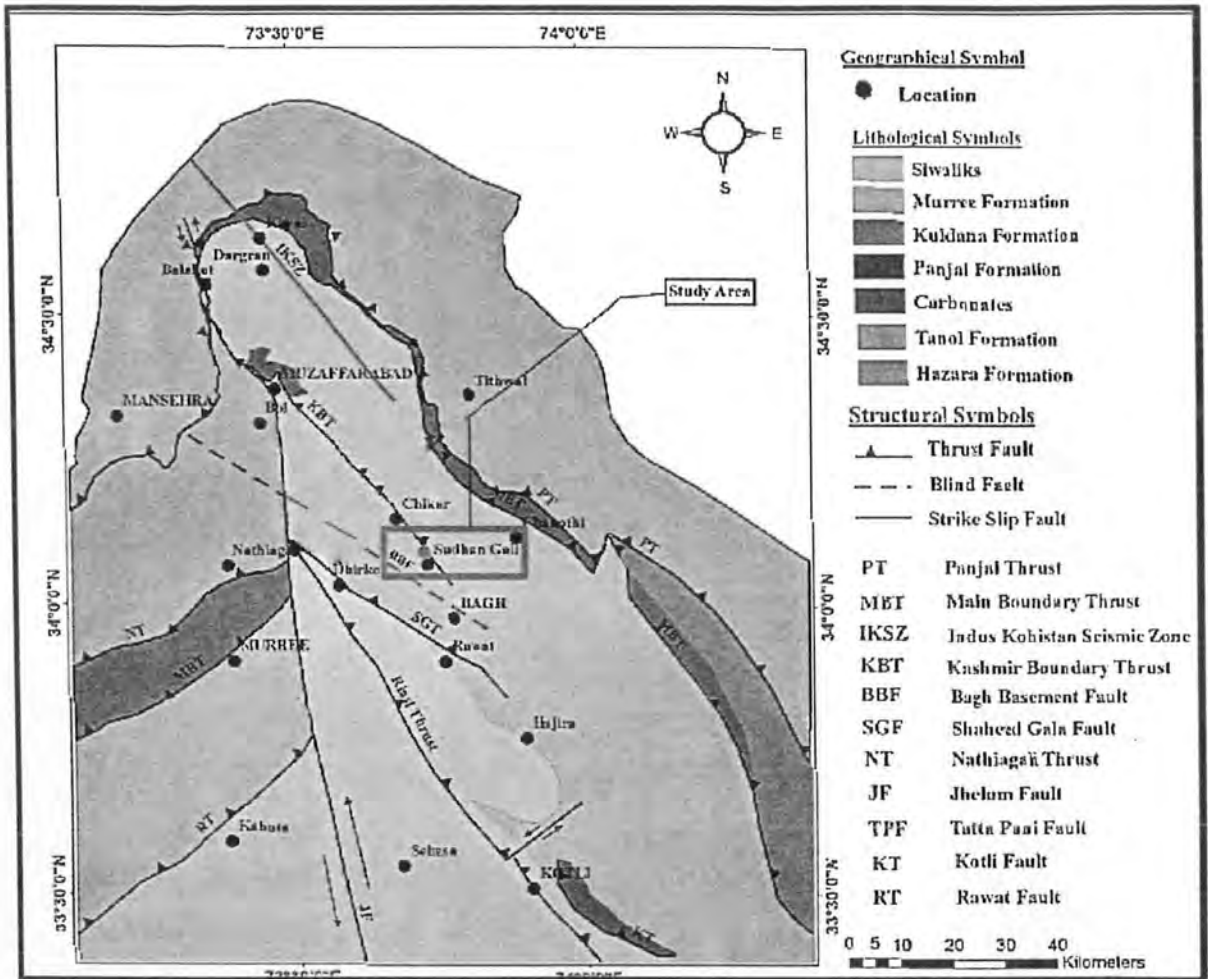


Fig.1.3 Geological and structural map of HKS after (Wadia, 1928) and (Khan & Ali, 1994).

Chapter 2

LITERATURE REVIEW

2.1 Previous work

The term "Landslide" is used to refer to down slope movement of debris, rock mass, or earth caused by the effect of gravity (Cruden & Varnes, 1996). Many other terms are being used with the term "landslide" including slope failure, mass movement etc. (Highland & Bobrowsky, 2008). Varnes (1978) suggested using the term "Slope failure" as it does not portray process. Brunsden and Prior (1993) used the term "mass movement" and differentiated this from mass transport being a process. Six types of landslides are classified by (Varnes 1978) based on material type and type of movement. Several other classification schemes are proposed by other researchers based on different parameters (Hung et al., 2001; Hutchinson 1988; Varnes 1978).

Geologically, the world's youngest and most dominating mountain systems are the Himalayas. They consist of the areas which are badly affected by slope movement's hazards in Pakistan (Kazmi and Jan 1997). According to Khan (2006) among the total worldwide distribution of landslides 30% of landslides occur only in the Himalayas.

Several researchers have studied the characteristics and distribution of landslides in Azad Kashmir that were caused by the disastrous earthquake of October 2005. Sato et al., (2007) analyzed the distribution of landslides caused by the 2005 Kashmir Earthquake. They described that the majority of the landslides occurred in the hanging wall block of the Muzaffarabad fault and a greater concentration of landslides is in Miocene Murree Formation. Kamp et al., (2008) generated landslide susceptibility map for the 2005 Kashmir earthquake affected region. They developed a spatial database based on Advanced Space borne Thermal Emission and Reflection Radiometer (ASTER) imagery and Geographical Information Systems (GIS). They evaluated multiple criteria to understand their control of triggering the landslides. They concluded that the landslides are clustered in certain zones related to event controlling parameters like deforestation, distance to fault, lithology and road network. Basharat et al., (2012) studied the Hattian Bala rock landslide which is the biggest landslide caused by 2005 Kashmir earthquake. This slope movement blocked two major streams of the area which are tributaries of the river Jhelum by forming two natural dams. They investigated the topographic, structural, and lithological control of this landslide and concluded that southeast plunging synclinal structures are controlling factors of this landslide. Bedding planes of rock units provided the slip surface of this landslide.

Earthquake deformation and ground shaking are also contributing factors to the reactivation of this mass movement. Basharat et al., (2014) studied the spatial distribution of landslides that were caused by the earthquake in 2005. The studied mass movements occurred in Neelum Valley, Muzaffarabad and Jhelum Valley and the Northeast Himalayas of Pakistan. They used Geographic Information Systems (GIS) to analyze the relationship between distributions of studied landslides using different factors, i.e., geological units, distance from an epicenter and fault and topographic features. They concluded that there is an increase in the intensity of landslide near the epicenter of fault. They described that concentration of landslides is high in the hanging wall side of Muzaffarabad fault. Basharat et al., (2014) studied a landslide initiated by the 2005 earthquake of Kashmir. They investigated the geometrical and geological parameters of these large-scale slope failures and concluded that various factors such as rugged topography, steep slopes and undercutting of slopes are major causes of these ground failures.

2.2 Use of Geophysical Techniques for Landslide Investigation

Many geophysical techniques are used to investigate slope failures and to depict the internal structure and mechanical properties of displaced material by portraying the physical properties of slope forming material (Jongmans & Garambois, 2007). Several geophysical methods such as Seismic survey, geoelectric methods, Ground Penetration Radar (GPR) and Gravity Survey are used to understand the characteristics of landslides. The Electrical Resistivity Tomography (ERT) method, which works on the principle of measurement of the electrical resistivity values and their distribution in the subsurface, is largely being used to investigate landslides (Perrone et al., 2014). 2D and 3D ERT are widely used to understand the geometry and failure mechanism of landslides. Many scientists have used multiple geophysical techniques to study the characteristics of slope failures. Merritt et al., (2014) developed a 3D ground model of an active and complex landslide system in North Yorkshire, UK. They studied the landslide using integrated techniques i.e., 3D ERT, Borehole logging and remote sensing. This integrated study helped to analyze the lithology, subsurface structure and geotechnical properties of the studied landslide which was not achievable using only a single method of investigation. Kristyanto et al., (2017) investigated a landslide in Cianjur, West Java using 1D and 2D ERT. They identified two boundaries in soil based upon the resistivity contrast between the layers and regarded them as slip surfaces. Based on resistivity variation, the upper layer was demarcated as clayey soil and bottom layer as sandy soil.

2.3 Use of Geotechnical Techniques for Landslide Investigation

The intrinsic ability of the soil to withstand the occurrence of mass movement and/or landslides is known as soil Atterberg limits. Atterberg limits are influenced by a variety of intrinsic soil characteristics, although clay and organic matter content are the most significant (Hemmat et al. 2010). Quantifying physical characteristics such bulk density, hardness, wetness, and resistance can help us understand the soil Atterberg limits and how weathering processes work. Landslide resistance and sensitivity are indicated by soil Atterberg limits based on seasonal dynamics of rainfall, infiltration, overland flow, and topography.

In hill-range landscapes all over the world, Atterberg limits and related soil physio-chemical characteristics are crucial for spotting places that are vulnerable to catastrophic landslides (Heshmati et al. 2011). Numerous researchers have discovered that the Atterberg limits, which express the mass ratio of water-to-soil, indicate soil moisture content. For the research of landslide aspects, soil parameters have been assumed to evaluate the stability, consistency, and behaviour of soils (Kitutu et al. 2009). Landslides are greatly influenced by soil Atterberg parameters such as soil water content, mineral content, permeability, and porosity variations (Heshmati et al.2011;Kitutu et al. 2009).

Chapter 3

LANDSLIDE TYPES AND CAUSES

Landslide is a natural phenomenon in which different earth materials move down slope under the influence of gravity (Fig 3.1). These materials involve rock, soil, debris, organic material, landfill deposits or a mixture of all these (Cruden and Varnes 1996). This movement may occur by sliding, falling, toppling, spreading, or flowing. Generally, landslides occur in areas with high topographic relief, but they can also take place in areas with low topographic relief. Classification of landslides is based upon the mode of slope movement and the type of involved material. Landslides are a complex geological phenomenon that is controlled by a variety of factors.

3.1 Morphology of Landslide

A landslide mass includes various elements i.e., crown, scarp, foot, toe, slip surface, head, and cracks as shown in (Fig 3.1). These terms are defined by (Cruden and Varnes 1996).

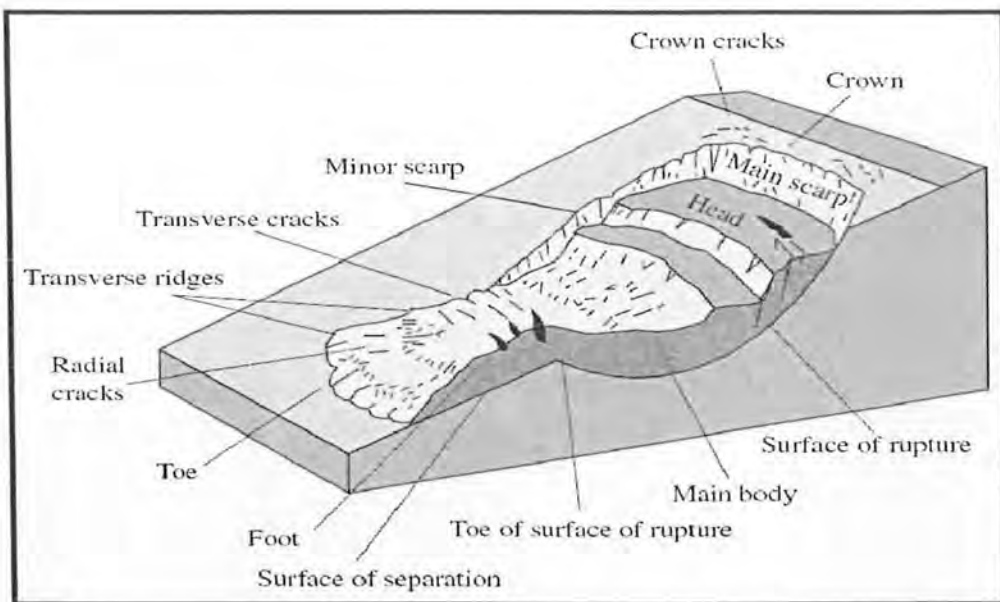


Fig. 3.1 Cross sectional diagram of a landslide illustrating landslide geometry (Varnes, 1978).

3.1.1 Crown

It is composed of undisturbed material which is still intact, and it is above the main scarp.

3.1.2 Main scarp

It is a nearly vertical surface set up at the upper edge of the sliding mass which is formed by the movement of displaced mass far from the stable ground.

3.1.3 Head

The head is the upper part of the sliding mass which is adjacent to the main scarp.

3.1.4 Main body

It is the displaced mass that lies over the slip surface, and it is bounded by main scarp on upper boundary and toe on lower boundary.

3.1.5 Toe

The toe is the lower and curved margin of the displaced material of a landslide, which is the far away from the main scarp and present at the bottom of the landslide.

3.1.6 Slip Surface or Surface of Rupture

The slip surface demarcates the sliding mass from underlying stable ground. It acts as a sliding surface along which material slides down along the slope.

3.1.7 Flanks

The undisturbed grounds adjacent to the sides of the main landslide body are called flanks. If viewed from crown left or right flank are used to describe the flanks otherwise compass directions are preferred.

3.2 Types of Landslides

Landslide is categorized based on initiation mechanism i.e., how a landslide is initiated and what type of movement is involved to displace the material from its original position. Different factors such as type of slope, forming material, the slope gradient and the hydrological conditions of the area control the type of landslides. Varnes (1978) divided landslides into six subclasses which include slides, spread, falls, flows, topples and complex. The schematic diagrams of types of landslides classified by Varnes (1978) based on material type and type of movement are shown in (Fig. 3.2).



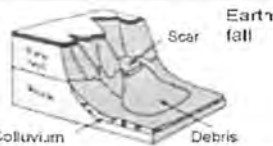

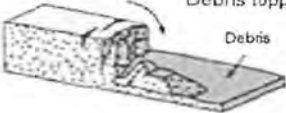

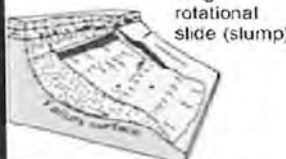
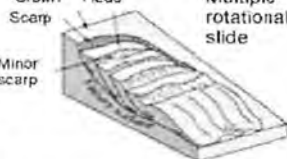
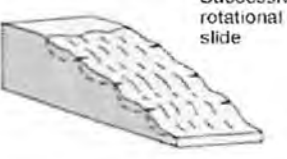
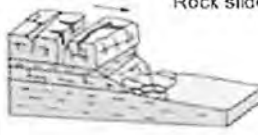


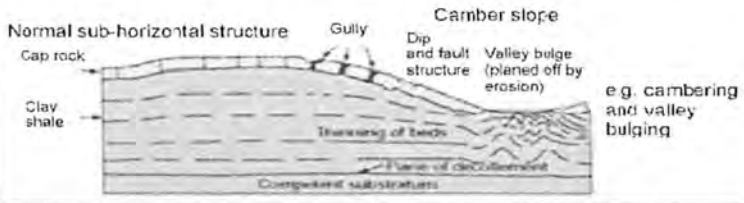





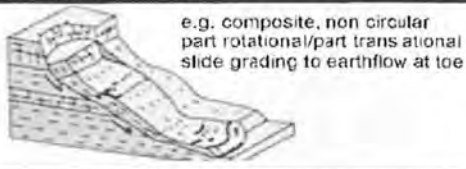
Material		ROCK	DEBRIS	EARTH
Movement type				
Falls		 Rock fall	 Debris fall Scree Debris	 Earth fall Colluvium Debris
		 Rock topple	 Debris topple Debris	 Earth topple Cracks Debris cone
Slides	Rotational	 Single rotational slide (slump)	 Multiple rotational slide Crown scarp Head Minor scarp	 Successive rotational slide
	Translational (Planar)	 Rock slide	 Debris slide	 Earth slide
Spreads				 Earth spread
Flows	 Solifluction flow (Periglacial debris flows)	 Debris flow		 Earth flow (mud flow)
Complex	 e.g. Slump-earthflow with rockfall debris		 e.g. composite, non circular part rotational/part translational slide grading to earthflow at toe	

Fig. 3.2 Schematic diagram showing the types of landslides as classified by Varnes (1978).

3.2.1 Falls

Falls are sudden, downslope movements of rock blocks or fine-grained material that is detached from steep slopes without contact with any shear surface. The falling mass falls, rolls, or topples freely under the action of gravity. Falls occur worldwide mainly on slopes with higher slope angles and cliffs. Falls also occur along banks of water channels and in coastline areas having rocky material. The

movement of falling material may be extremely speedy as the material moves without being in contact with any surface. The velocity of falls is dependent on the angle of the steepness of the slope (Highland & Bobrowsky, 2008).

The triggering mechanism of falls could be physical weathering which includes expansion of rock joints by tree roots, frost action (freeze and thaw cycle), anthropogenic activities or ground shaking. The material of rock falls varies, depending upon the weathering activity. Effects of rock fall are catastrophic events on both humans and buildings resulting in the blockage of roads, destruction of infrastructure and loss of property and life. The rock fall hazard can be mitigated by several measures such as the construction of retaining walls along roads and railway tracks, installation of rock bolts on poorly jointed rock faces, covering of slopes by rock curtains and removal of loose rocks by blasting.

3.2.2 Topples

A rock or soil mass topples when the material is removed from the cliff, and it rotates along the base and moves outward and falls. Material involving topples can be rocks, debris, soil, or composite of these materials. The force of gravity applied by the weight of material upslope triggers toppling. This material may vary in size from small fragments to cubic meters. Topples occur throughout the world commonly in columnar jointed volcanic terrain, steep slopes or along the banks of river channels.

Depending on the travel distance of the material their velocity can be extremely slow to extremely rapid. Triggering mechanism of topples could be gravity exerted by mass located upslope, presence of water in joints which can lubricate the movement, freeze, and thaw cycle, differential weathering or steepening of slopes through excavation. Tackle forming material is usually in the form of slabs and results in the occurrence of catastrophic events leading to blockage of roads, destruction of buildings and loss of people lives. The hazard of topples can be mitigated by slope stability measures such as the installation of rock bolts and anchors and the prevention of seepage through the construction of drainage pipes (Highland & Bobrowsky, 2008).

3.2.3 Slides

The term "slide" denotes the movement in which rock mass or soil slides down along a ruptured surface. A distinct zone of weakness separates the sliding material from the underlying stable ground. When the shear strength of slope forming mass is reduced, the movement originates along the shear surface. The addition of water in cracks reduces the strength of slope forming material. As the material slides down its volume increases because another material is combined with the sliding mass which comes into the way. Slides are classified into two classes: rotational and translational slides.

3.2.3.1 Rotational Landslide

It is the form of landslide in which the slip surface is curved and sliding earth material moves along the concave upward rupture surface. Sliding material forms a spoon-like shape at the head of the landslide and movement is nearly rotational about an axis parallel to the slope. If a slide is rotational and is comprised of several failure planes which are curved, then it is termed as a slump. Rotational slides commonly occur in homogenous material and landfill deposits. Velocity may vary from extremely slow to moderate. They are induced by heavy or prolonged rainfall, rise in groundwater level, increase in level of water channels at the base of a slope which causes erosion and earthquakes. The rotational slide can severely damage infrastructure such as buildings and roads, the rate of movement is generally slow, so they are not life threatening. These slides can be mitigated by installing drainage pipes to expel water from the slope and by the construction of retaining walls.

3.2.3.2 Translational Landslide

In translational landslide material moves downward along a planar surface with no rotational movement and rolling. The surface on which sliding mass moves may be bedding planes, lithological discontinuities, faults, contact between rock and soil layers and in preexisting surfaces. In contrast to rotational slides, the material can be non-homogeneous varying from unconsolidated soil to rock slabs or both. Translational landslides are common and frequently occur throughout the world. The velocity of travel of translational landslides can be extremely slow to rapid depending upon the geometry of the slope. As the velocity increases the material may disintegrate and form debris flow. This type of landslide is triggered by intense rainfall, snowmelt, earthquakes, and anthropogenic activities such as undercutting slopes. Translational slides damage property and lifelines if velocity is slow, with an increase in velocity it can be life-threatening. The translational slide can be controlled by diverting the drainage from active slides to prevent reactivation. By constructing retaining walls and ground leveling the hazard of translational slides can be reduced.

3.2.4 Lateral Spreads

Spread is the type of mass movement which occurs mostly in flat terrain or an area with gentle slopes. In lateral spreads the upper layer composed of soil or rock moves over underlying softer materials i.e., silt, clay, or soil. This movement is further accompanied by the subsidence of a stronger upper layer into a weaker lower layer. Spreads occur worldwide mostly in areas where liquefiable soils are present. The velocity of travel may vary but they can move rapidly if followed by an earthquake. The triggering mechanism of spreads involves liquefaction of weaker lower layers by seismic shaking, overloading of

ground above weak material and saturation of underlying mass by groundwater percolation of precipitation.

3.2.5 Flows

In this type of mass movement material moves spatially, and the shear surface is closely spaced, Short-living and usually remains unpreserved. Flows are further subdivided into the following types based upon failure mechanism.

3.2.6 Debris Flow

This type of mass movement involves rapid movement of the mass. A mixture of soil, organic matter, clay, and debris combines with water to form a mixture of water and slope forming material and moves downslope. These are caused by intense surface runoff or by heavy rainfall that erodes and mobilizes the unconsolidated soil or rocks present on slopes. Sometimes rotational or translational slides get velocity and transform into debris flows. In Debris flow less than 50% soft material is present. Debris flows occur worldwide and are common in gullies and canyons. They are triggered by heavy rainfall or snowmelt, and heavy surface water flow. Debris flow is disastrous as they move rapidly and swipe away the structures which come along their way. Check dams should be constructed over water channels to mitigate the debris flow hazard.

3.2.7 Debris Avalanche

Debris avalanche is a type of flow in which an open slope collapses and collapsed material moves away from the slope rapidly. It occurs mostly in steep terrain and in steep volcanoes.

3.2.8 Earth Flow

Earth flows occur commonly in silt, clay or fine-grained soils located on steep or gentle slopes. They can also occur in weathered or clay-bearing bedrock. Slides can also evolve into earth flows. A strong internal deformation is formed in material involving earth flow causing plastic flow. Earth flows occur in areas where weathered rock or fine-grained soils are present in the subsurface, Intense rainfall, the decline of the water table, and erosion of the valley bottom causes earth flows. Earth flows are distinct from debris flow as they contain about 50% finer material i.e., clay and silt.

3.2.9 Creep

It is the slowest type of mass movement which is also termed as slow earth flow which involves slow and steady downslope movement of material. When the internal shear strength of the material is sufficient to cause internal deformation but cannot initiate the failure creep occurs. Creep is a common

type of landslide which occurs mostly in fine-grained materials, and it has the potential of damming. Drainage of water channels and slope adjustment can be used to control creeps.

3.2.10 Complex Slide

A complex slide is formed when more than two types of landslides are combined. Usually, failure initiates as a single type of failure but the addition of other mechanisms lead to the formation of complex slides such as the addition of water into a debris slide results in formation of debris flow.

3.3 Factors Causing Landslides

Landslides are caused by various factors; they might be natural or human induced. A landslide occurs when driving forces (forces acting on the material to move along the slope) are greater than resisting forces (which help material to remain on the existing slope). Various factors play their role in increasing the driving force to act on a slope which induces a landslide. A single factor does not affect the landslide phenomena as it is a complex phenomenon. Water is one of the most important parameters to reduce slope stability. Due to prolonged or intense rainfall moisture content of slope forming materials is increased which adds weight to the materials. This increase in weight leads to a decrease in resisting forces which ultimately enhances driving forces acting on a material. As a result, the material tends to move along the slope and slope failure occurs. Saturation of soil, an increase in the water table and pore pressure also has a negative impact on slope stability.

Hill cutting is one of the anthropogenic activities which help landslides to induce. In many areas of the world, landslides are caused by hill cutting. When a slope is undercut for the development of infrastructure i.e., construction of roads and buildings, a slope gets steepened and its stability decreases. Deforestation is also one of the significant causes of landslides. Tree roots enhance soil compaction and thus prevent soil erosion. Areas that have a higher ratio of vegetation cover or forest have a low frequency of landslides. Human activities are responsible for the reduction of these natural resources which also results in an indirect reduction of soil strength and makes the area prone to landslides. Loss of vegetation on a slope helps increase in erosion rate which results in slope failure.

3.3.1 Triggering Factors of Landslides

The factors which contribute to triggering a landslide are known as triggering factors of a landslide which include Human-induced factors, natural factors, geological factors etc. Human-induced factors are among the most common factors which are involved in triggering a slope failure. Sometimes this activity makes the area unstable on a large scale which results in the occurrence of devastating mass

movements. Activities related to infrastructure development are one of the major human-induced factors which help to trigger a landslide. When the toe of the slope is excavated for construction purposes, slope gets steepened, and it provides a favorable condition for a slope failure.

Natural factors i.e., earthquakes, climate change, prolonged rainfall, and weathering also contribute to initiation of landslides. The long-lasting variation in the atmosphere can significantly affect slope stability. A general reduction of rainfall lowers down the level of the water table and decreases the mass of soil which results in the reduction of freeze thaw activity. As the water level rises with prolonged saturation or by rainfall in an area, this may increase both erosion and freeze and thaw cycle. The freeze and thaw cycle causes a reduction in the strength of slope materials. Occasionally, both quick snowmelt and the prolonged saturation cause increment of slope stability problems in the area. The structure of soil or rock gets weakened by the weathering process of nature which results in a huge production in the landslide-prone materials. This process of disintegration involves both physical and chemical weathering. However main reasons which are contributing to slope instability are inherent (weak soil structure), variable (heavy rainfall, snowmelt, groundwater level fluctuation), transient (seismic-activity or volcanic-activity) and environmental situations (drainage types and weather pattern of the area).

3.3.2 Geological Conditions

Many geological parameters i.e., lithology, bedding planes, joints, faults are involved in the occurrence of landslides. Lithology plays a vital role in triggering landslides during an earthquake. Hard and intact rocks are less prone to landslides as compared to highly jointed and fractured rocks or loose sediments. Swelling clays are more prone to the occurrence of landslides after heavy rainfall. The strength of the materials is directly related to the occurrence of landslides. Various discontinuities such as bedding planes, joints, faults, and sheared zones act as a sliding surface for the landslides.

3.3.3 Topographical Conditions

Topographical conditions involve different factors which are dependent upon the topography of an area such as slope angle, slope aspect, the curvature of the slope etc. These are contributing factors to the distribution of landslides in an area. An increase in slope angle or steepening of slopes by natural or man-made causes plays an important role in the occurrence of a slope failure. When a slope gets over steepened gravitational forces on slope increase, which leads to a decrease in resisting forces and addition of driving forces which result in a landslide. Other topographical parameters i.e., curvature and aspects also contribute to slope failures.

3.3.4 Hydrological Conditions

Rainfall is one of the most common factors which is involved in the distribution and initiation of mass movements throughout the world. Excessive precipitation, prolonged rainfall, snowmelt, changes in the groundwater table, rise in water reservoirs and coastlines and floods are the hydrological factors involved in the initiation of landslides (Highland & Bobrowsky, 2008). Water from the different sources enters the ground through cracks and fissures and increases the ground water table. Thus, as a result, material lying on slope gets saturated. As this slope forming material gets saturated resisting strength of the material is decreased and driving force is increased due to the addition of weight through water. This unbalances the equilibrium of slope and slope failure takes place.

3.3.5 Structural Conditions

Structural conditions of an area also contribute to the occurrence of slope failures. Structural discontinuities such as bedding planes, joints, fractures, faults, and shear zones make the area more vulnerable to landslides. The placement direction and the strength of these structural discontinuities also control the stability of slopes. The presence of these structural discontinuities represents the weak zone in slopes. As a result of these weak zones, the material can easily slide or move over these planes of weakness.

Chapter 4

METHODOLOGY AND RESOURCES

This chapter discusses the methodology and the materials used for conducting the research work. The methodology and resources used for the investigation of Sarbala landslide are like those described in the existing literature. A detailed account of methods followed, and resources used are described under the following sections. (Fig 4.1) gives a summary of work flow adopted for this investigation of Sarbala landslide.

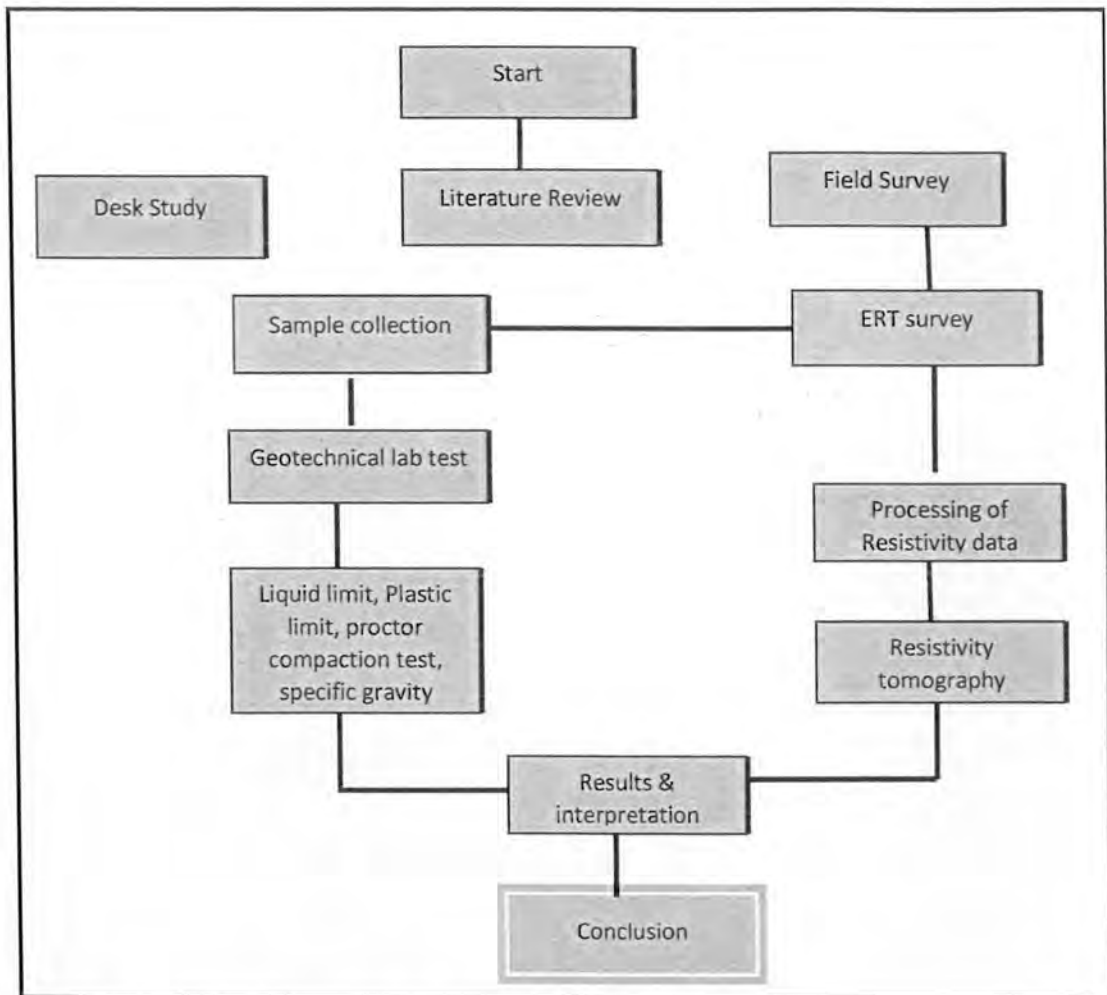


Fig. 4.1 Schematic flow chart of the research methodology.

4.1 Electrical Resistivity Tomography (ERT)

Electrical Resistivity Tomography (ERT) is a widespread emerging subsurface imaging technique. This technique has a wide-ranging application in civil engineering, hydrogeology, environmental investigation, geophysics, and sub surface geology. As compared to the conventional Vertical electrical Sounding (VES) technique that only gives one-dimensional coverage, the continuously growing ERT technique gives two-dimensional coverage and has a better distribution of subsurface resistivity (Loke 1999). After its evolution in 1970 due to continuous advances of the multi-electrode array, acquisition systems, and advanced algorithms this technique has denoted itself best for shallow structures (faults & folds), in the identification of subsurface strata, and solute transport. The ERT technique is based on the injection of a defined amount of electric current to the ground by two current electrodes. The amount of resistance faced by the current from the subsurface soil conditions (presence of fractures, material type, and moisture content) is measured by two electrodes called potential electrodes. ERT works on the principle of the flow of electric current (Loke, 1999). One electrode is called source which is connected to positive terminal and other is called sink that is connected to negative terminal. Because of potential differences, the current is required to flow along paths leading from source to sink.

Interpretation of Resistivity data depends on the fact that the underlying geological layers appear in a series of isotropic, homogeneous, and horizontal strata of fixed thickness (Koefoed, 1979). Interpretation of true resistivity values of the subsurface strata in terms of geology and hydrogeology is not possible, due to wide parallel resistivity ranges of rocks. But by using geological information of the area different zones of resistivity can be marked to specific geological and divisions. Also, these values are the combined effects of the resistivity of subsurface layers and the measured resistivity is apparent resistivity. The apparent resistivity is obtained from the ratio of measured voltage to the applied current. The apparent resistivity values will be changed by the changing spacing and the positioning of four electrodes (Fig 4.2).

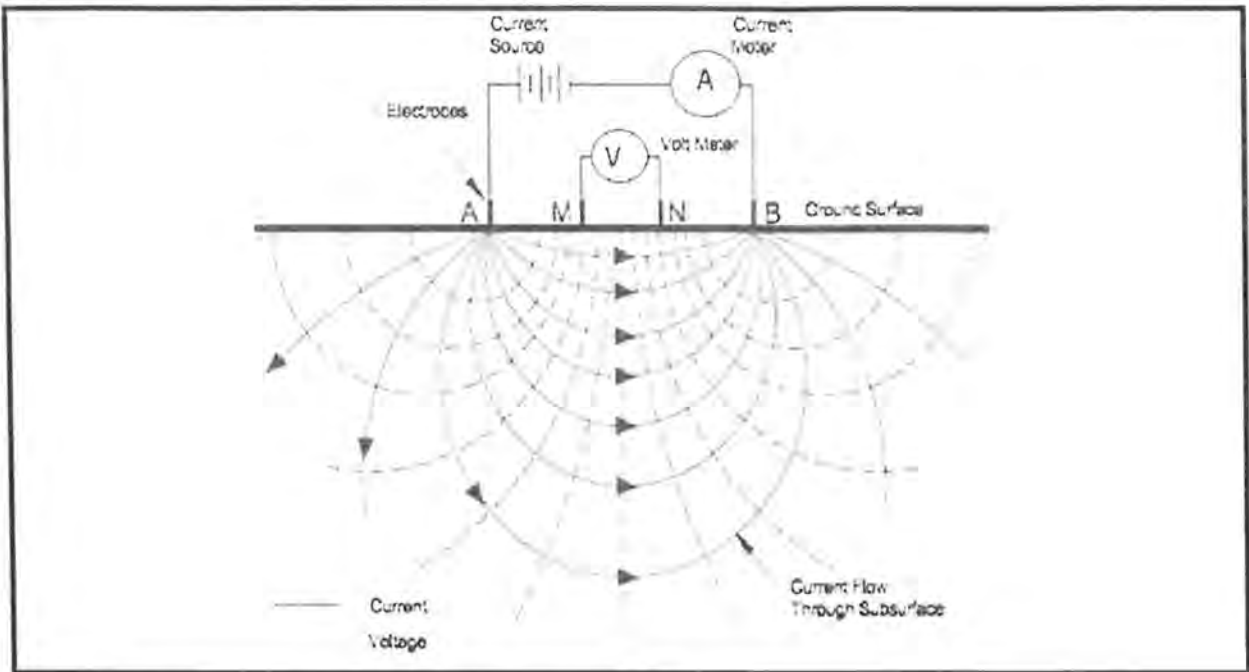


Fig.4.2 ERT Survey procedure and current flow pattern (Marescot et al., 2009).

4.2 Relationship between Resistivity and Geology

The rocks and soils in the subsurface exhibit a wide range of resistivity which is controlled by the type of rocks, type of minerals, soil type, fractures, porosity, and water content. To get a geological picture from a resistivity image it is essential to have a solid understanding of the local geology, as well as the resistivity ranges of different underlying material types. The resistivity values of metamorphic and igneous rocks are typically high. The rocks' resistance varies according to the degree of fractures and the proportion of fractures that are filled with water. The rock conductivity is determined by the fluid conductivity (and its chemical composition), the amount of water present, porosity, and permeability. However, because of differences in mineral compositions and pore geometries, resistivity does not always correspond to porosity even in the same type of rock. Normally, sedimentary rocks exhibit low resistivity as they are more pore spaces that are covered by water (Todd & Mays, 2004). Fresh groundwater and saturated soils have much lower resistivity values (Zohdy et al., 1974). There is always considerable overlap in resistivity values as resistivity values are controlled by various factors such as porosity, the amount of water saturation and the number of dissolved salts. Resistivity of some common rock types and soil are given in (Fig 4.3).

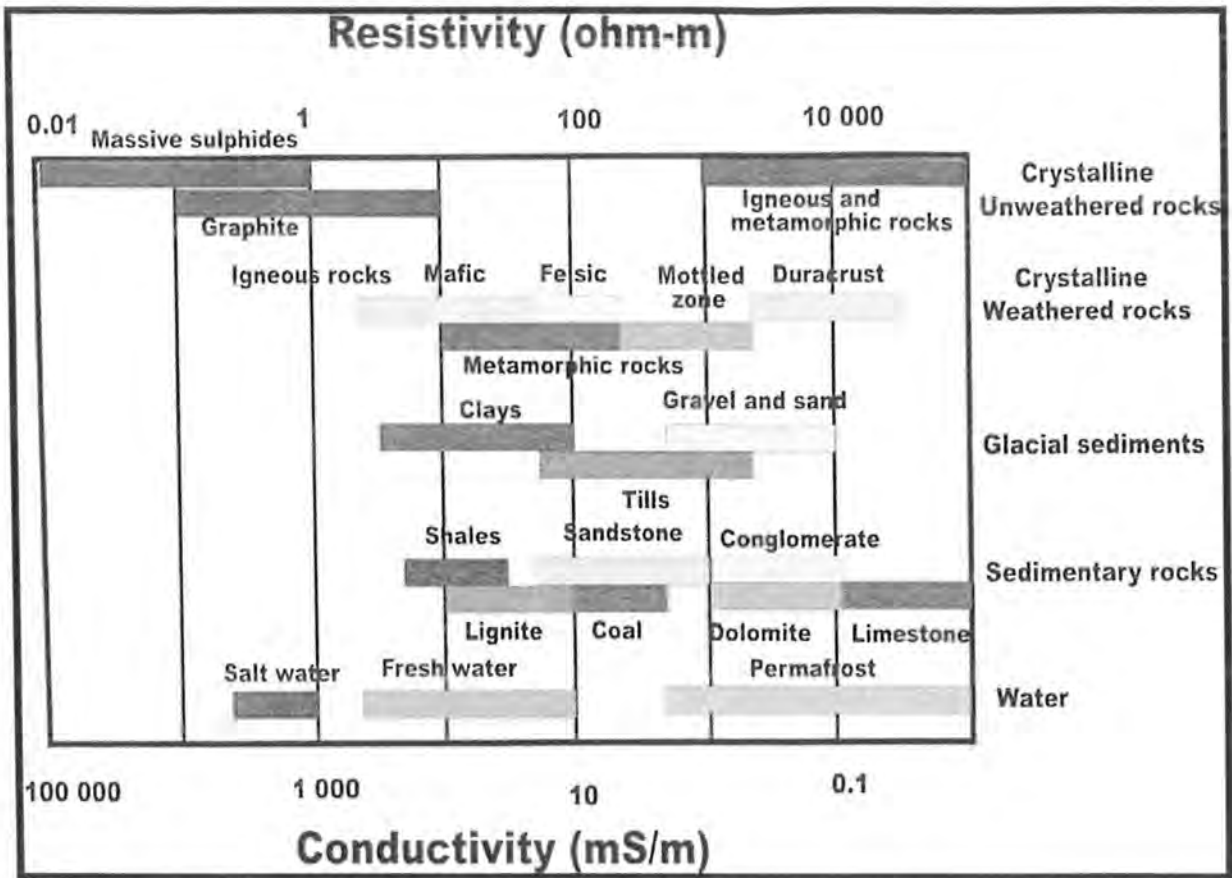


Fig. 4.3 Showing the Resistivity ($\Omega.m$) and Conductivity (mS/m) values of common rock types and aquifers (Palacky, 1991).

4.3 Data Acquisition and Processing

4.3.1 Instrumentation

The Terameter SAS 4000 (Sweden) ABEM instrument, along with its accessories such as hammers, stainless electrodes, cables, and measuring tape, was used to collect data in the area (Fig4.4). In this configuration, for subsurface depth coverage, the distance between the electrodes was proportionately increased. Pair of electrodes were used to measure the potential difference that was created after applying current. The obtained data were processed using the IPI2WIN (2008) iteration software. The software uses data from a single point's 1D geoelectric measurements to automatically analyses the information with the least amount of error in order to determine the depth, thickness, and true resistivity of the underlying layers.



Fig.4.4Electrical resistivity method Equipment: (a) Terrameter SAS 4000, (b) selector and (b1 and b2) connectors, (c and c1) cable and connectors, (d)electrodes, (e) cable-electrode connectors and (f) battery supply.

4.3.2 Electrode Configuration

Electrode configuration means the arrangement of electrodes used in the measurement of resistivity data. Several arrangements of electrodes depending upon the type of problem, practical possibilities of elimination of measurement in the field, the complexity of the investigation, possible shortcomings of measurement and interpretation are being used. The most used configurations are Wenner, dipole-dipole and Wenner-Schlumberger.

4.3.2.1 Wenner Array

The Wenner configuration consists of equally spaced electrodes and that distance remains fixed throughout the survey. The two inner electrodes are potential electrodes, while the two outer electrodes are current electrodes. This method gives good lateral coverage but after every reading all four electrodes are shifted to the next locations the deepness of infiltration is reciprocal to split between

electrodes. Wenner arrangement is more sensitive to changes in the subsurface resistivity that occur vertically and less sensitive to changes that occur horizontally (Barker, 1979).

4.3.2.2 Schlumberger Array

The Schlumberger array has four electrodes as well. The two inner electrodes are potential electrodes, whereas the two outer electrodes are current electrodes. However, in this setup, the current electrodes are kept moving after each reading while the potential electrodes are kept fixed. This array is more sensitive to water and vertical changes in lithology but less sensitive to horizontal homogeneities in sub surface.

4.3.2.3 Dipole-Dipole Array

The dipole configuration is different from both Wenner and Schlumberger configurations. It consists of four electrodes the only difference is that potential electrodes are kept away from current electrodes. It is not necessary for potential electrodes to be placed inside current electrodes. The dipole-dipole arrangement is very sensitive to the contrast in horizontal resistivity changes but is substantially less sensitive to the contrast in vertical resistivity changes. Therefore, it is beneficial to map vertical structures, such as cavities and dykes, whereas mapping horizontal structures like sedimentary layers or sills is generally less effective.

4.4 Geotechnical Approaches

4.4.1 Laboratory Soil Testing

The soil sample taken from the selected landslide of the study area was carried to the engineering laboratory where different soil tests were performed on them to assess the soil engineering properties to categorize the failure mechanism and to determine the physical and mechanical characteristics of the landslide from which that sample was collected.

4.4.2 Soil Test

On the soil sample of the landslide, different laboratory tests were performed which are shown in Table 2.1

Table 2.1: List of Laboratory tests performed and standards.

Laboratory Test	Standards
Sieve Analysis	ASTM D422
Liquid Limit by Casagrande method	ASTM D4318
Plastic Limit	ASTM D4318
Specific Gravity	ASTM D854; D5550
Proctor compaction test	ASTM D698

4.4.3 Sieve Analysis

A sieve analysis, also known as a gradation test, is a method of assessing a particle size distribution. Grain size analysis is classified into two categories:

- Mechanical analysis
- Hydrometer (or fine) analysis

Mechanical analysis is used to calculate particle sizes and relative distributions for particles larger than 0.074mm by stacking sieves on top of one another, adding a given weight of soil to the top sieve, then shaking the sieve in a particular way to allow the soil to fall through the stack (Fig 4.5).

A sieve is formed out of a 2-inch-deep, 8-inch-diameter metal ring with a wire mesh on the bottom, often made of brass. The sieve is assigned a number that represents how many apertures there are on a screen's surface per linear inch; for example, the United States Bureau of Standards No.4 sieve has four 0.187-inch openings per inch.

4.4.3.1 Apparatus

- Set of sieves containing sieve No. 3, 4, 10, 20, 40, 60,100, and 200.
- Pan and lid, sieve shaker, Balance

4.4.3.2 Procedure

- Set the sieves with the largest sizes at the top and gradually decrease the size.
- Pour the sample into the sieve.
- Place the sieves on a shaker for 3 to 4 minutes.
- Remove the sieve set from the shaker and weigh the retained mass on each sieve.

Calculation

$$\text{Percentage retained} = \frac{\text{Mass of soil retained}}{\text{Total mass of sample}} \times 100, \quad (1)$$

$$\text{Percentage passing} = 100 - \text{cumulative percent retained}. \quad (2)$$

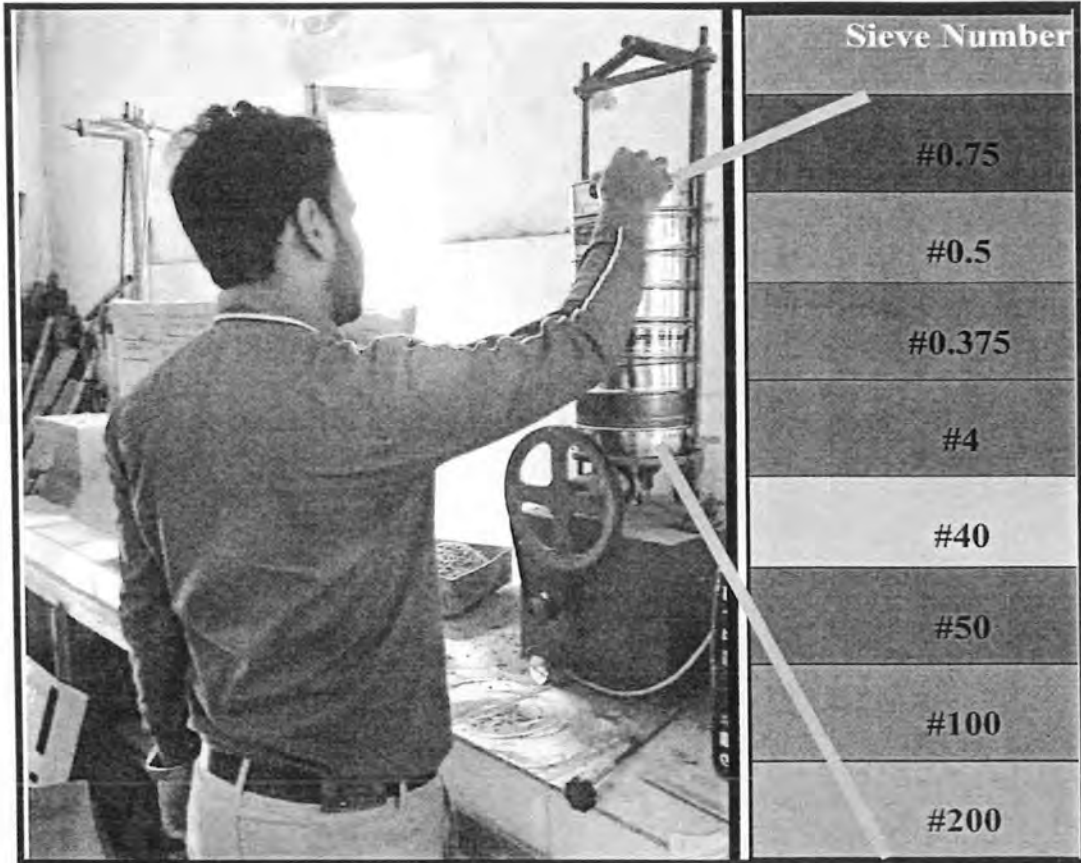


Fig. 4.5 Different mesh sizes are arranged on shaker for gradation of soil sample.

4.4.4 Atterberg Limits

Atterberg limits include L.L, P.L, and plasticity indexes that are calculated using the ASTM standard.

4.4.4.1 Liquid Limit (LL)

When the wetness of the soil changes from liquid to plastic or from plastic to liquid, the percentage moisture content of the soil changes.

4.4.4.2 Plastic Limit (PL)

In a standard test, the plastic limit is the water content at which a soil-water paste changes from a semisolid to a plastic consistency when rolled into a 3mm diameter thread. The cohesiveness of the soil will be disturbed by a small increase in moisture above the P.L.

4.4.4.3 Plasticity Index (PI)

A high plasticity index implies that there is too much clay in the soil. When the PL is more than or equal to the LL, it has no value. The procedure used to calculate the liquid limit and plastic limit of a soil are as follows.

4.5 Liquid Limit (Casagrande Method)

4.5.1 Apparatus

Casagrande, grooving tool, Balance, Spatula, Evaporating dish, Container, Oven, and No. 40 sieve (Fig 4.6)



Fig. 4.6 Apparatus for liquid limit by Casagrande method.

4.5.2 Procedure

- The 250 g of oven-dried sample after passing through NO.40 sieve and added 15 to 20ml water was taken.
- Then thoroughly mixing was carried out till it becomes a thick paste.
- Then the device cups filled with a soil sample and smooth its surface.
- After that cut the center of soil with the help of spatula so its bottom becomes visible.
- Give the number of blows with the device until half of the cut joins.

- The interval between 2 blows was second.
- The 20 to 30 g sample was used for moisture content.
- Was repeated 3 to 5 times.

4.6 Plastic Limit

- The 10 to 20 g of soil after passing through sieve NO.40 and added 2 to 3 ml water was taken.
- Take 8g of paste and form a small ball.
- Then press it with palm on glass plate until it gets diameter of 3mm.
- Then take a sample for moisture content.

4.7 Specific Gravity

Sometimes it is essential to relate the density of soil solids to the density of water. This assessment is expressed as a proportion, and it is stated as the specific gravity of soil solids. Many interactions, such as void ratio, porosity, and particle weight analyses, as well as consolidation and compaction, are solved using specific gravity in combination with soil moisture and unit weight.

4.7.1 Apparatus

Volumetric flask 250 ml (Pycnometer), Balance, Thermometer, Water, Sieve NO.10.

4.7.2 Procedure

- Washed the pycnometer and weighed it as W1.
- The 250g of oven-dried soil passing sieve No.10 was taken in pycnometer and weigh it as W2.
- Then fill the flask up to the mark.
- Then remove any bubbles present in the flask.
- After that weight the flask with soil and water as W3.
- Then unfilled the flask and clean it thoroughly.
- Finally, fill the flask up to the spot with water and weigh it as W4.

Calculation

To determine the specific gravity in the laboratory, the volume of soil solid and water are taken the same the equation can be written as.

$$\text{specific gravity} = \frac{W_2 - W_1}{(W_4 - W_1) - (W_3 - W_2)} \quad (3)$$

4.8 Proctor Compaction Test

In order to determine the maximum dry density and optimum moisture content of a given soil, the Proctor compaction test was performed. The test is named after Ralph R. Proctor, who demonstrated in 1933 that a soil's dry density for a given compactive effort depends on how much water it contains at the time of compaction. His original test is known as the standard Proctor compaction test; however, his test was later updated to the modified Proctor compaction test.

4.8.1 Apparatus

- A mould of diameter 4 in for standard proctor and diameter of 6 in for modified proctor test.
- A hammer that has specific weight.
- Water.
- Soil sample
- Moisture container.
- Balance.
- Oven.

4.8.2 Procedure

- Oven dried soil sample is taken and weighed.
- The weight of mould is noted without collar of mould.
- The sample is placed in a tray and 5% moisture is added into the sample and mixed thoroughly.
- For standard proctor test the sample is placed in the mould in three layers with 25 blows after each layer.
- The collar is removed, and the surface of mould is smoothed using spatula.
- Sample with mould is weighed and noted.
- Some amounts of sample are placed in container for moisture and weighed.
- The process is repeated several times until the weight starts to decrease by increasing moisture.

Calculation

Using the value taken during the compaction test the graphs are made from which the value of optimum moisture content (OMC) and maximum dry density (MDD) are calculated.

Results

5.1. Sarbala Landslide

The landslide affected area comprised of road, trees, water pipelines and farmland were damaged due to this mass movement section of the road having a length of 200 meters was affected by the landslide which is the road connecting district Bagh to Muzaffarabad and Hattian (Fig 5.1). As inferred from the geology and morphology of the study area the landslide seems to be activated due to multiple factors.

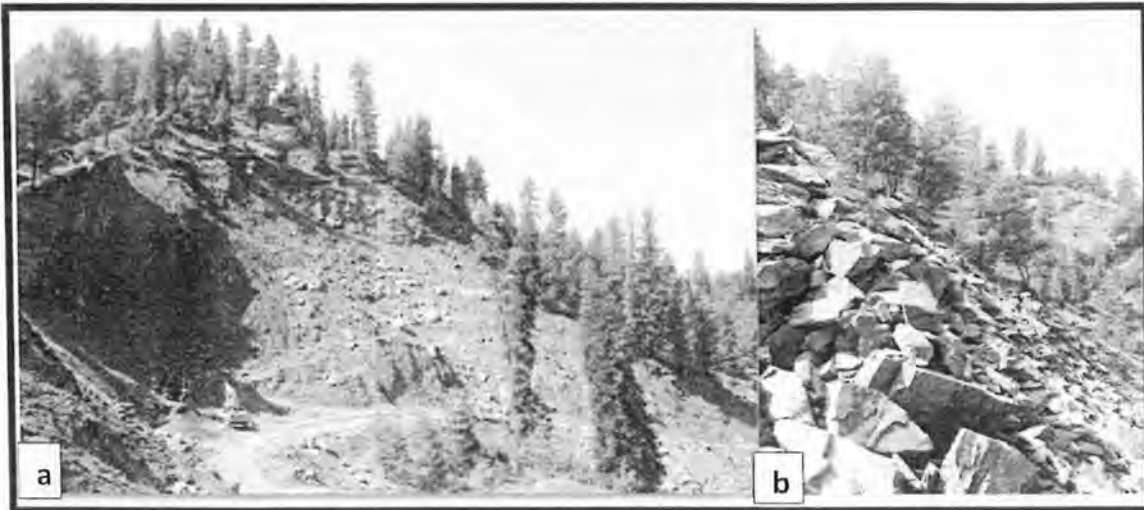


Fig. 5.1 Massive land deformation and tilting of trees caused by Sarbala Landslide.

5.1.2 Landslide characteristics

Sarbala landslide occur in Murree Formation. The Sandstone is exposed on the upper part of landslide which is highly fractured, and clays are exposed at the right and left flanks of landslide and adjacent area. The total calculated area of this landslide is 53,650 square meters. The landslide is divided into depletion zone, transition zone, and deposition zone. The characteristics of Sarbala landslide are as follows.

5.1.2.1 Main Scarp

The main scarp of the Sarbala landslide is composed of fractured and weathered sandstone and clays of the Miocene Murree Formation (Fig 5.2). The main scarp of landslide is 340-350 m long.



Fig.5.2a Main scarp of landslide., b -Main scarp at the head of the landslide near road, c -Fractured sandstone of the Murree Formation exposed at main scarp.

5.1.2.2 Cracks

Cracks are well developed in the body and crown of Sarbala landslide. The cracks developed in the Sarbala landslide are tensional cracks which affect the stability of landslide. These cracks are developed due to the loss of soil strength. The length of these cracks measured ranges from 02 meters to 12 meters and the width is 0.4cm to 2 meters. The series of parallel to sub-parallel tensional cracks are present at the Crown of landslide (Fig. 5.3). Water percolates through these cracks, increasing the weight of soil and rock materials and increasing the possibility of triggering a landslide. When the slope was exposed to heavy rainfall, the detrimental effect of cracks on soil displacement became more apparent, resulting in a rapid and massive landslide. Moreover, runoff water flows into these cracks thus resulting in a reduction of effective stress of soil mass.

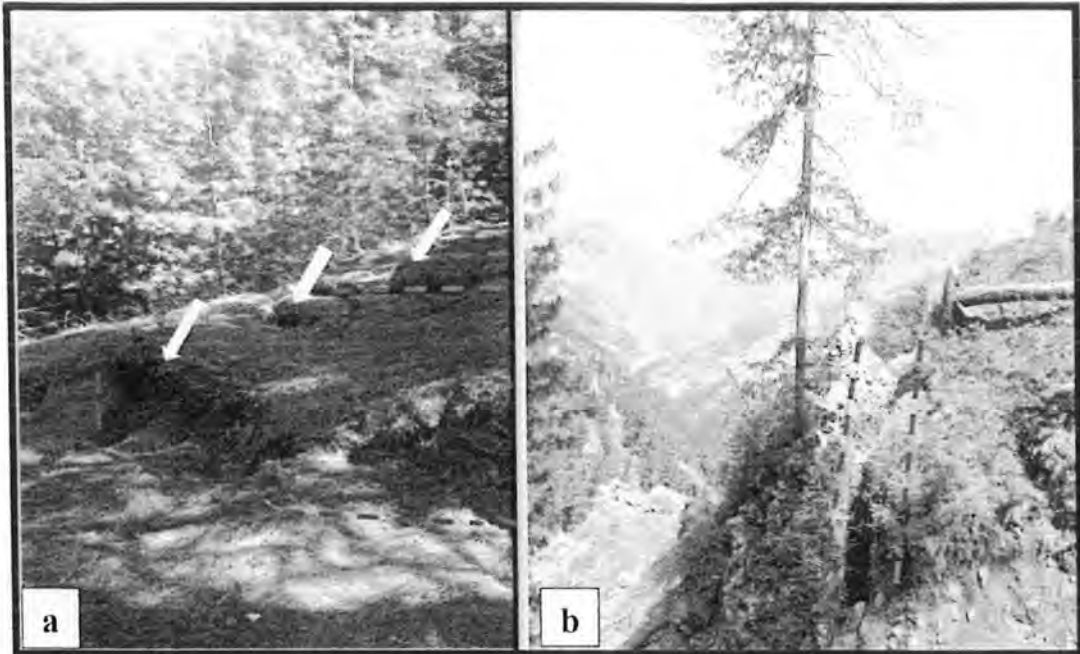


Fig.5.3 a &b - Slippage of a block of soil due to cracks at crown.

5.1.2.3 Depletion zone

Sarbala landslide depletion zone is 35-40 m long and 180-185 m wide. The depletion zone covers an area of approximately 6,100 square meters (Fig 5.4). Clays and fractured sandstone dominate the depletion zone of Sarbala landslide. Water seepages are also present in depletion zone. The scrap appears to have formed because of the detachment of sandstone beds along the nearly vertical surface. The study area rock mass is a highly jointed and fractured rock body.

5.1.2.4 Transition zone

The transition zone of Sarbala landslide consists mainly of clays material and large boulder beds of sandstone. Transition zone is showing rotational earth slide within clays. The length of the transition zone is 195-200 m, and the width is approximately 145-150m (Fig 5.4). The area covered by the transition zone of the land slide is 23,440 square meters. The slope angle measured in this zone was 40-50 degrees.

The volume of the landslide has increased due to the accumulation of rock material and large boulders along the down slope.

5.1.2.5 Deposition zone

The deposition zone of the Sarbala landslide is 235-240 m long and 100-105 m wide. Sarbala landslide deposition zone consists of large sandstone beds with rock avalanche debris in the lower part of the

landslide (Fig 5.5). The volume of the landslide has increased due to the accumulation of large boulders and rock debris along the down slope. The calculated surface area of the deposition zone is approximately 24,110 square meters. The deposition zone consists of sandstone boulders and rock material. The total area of landslide is calculated to be about 53,650 square meters.

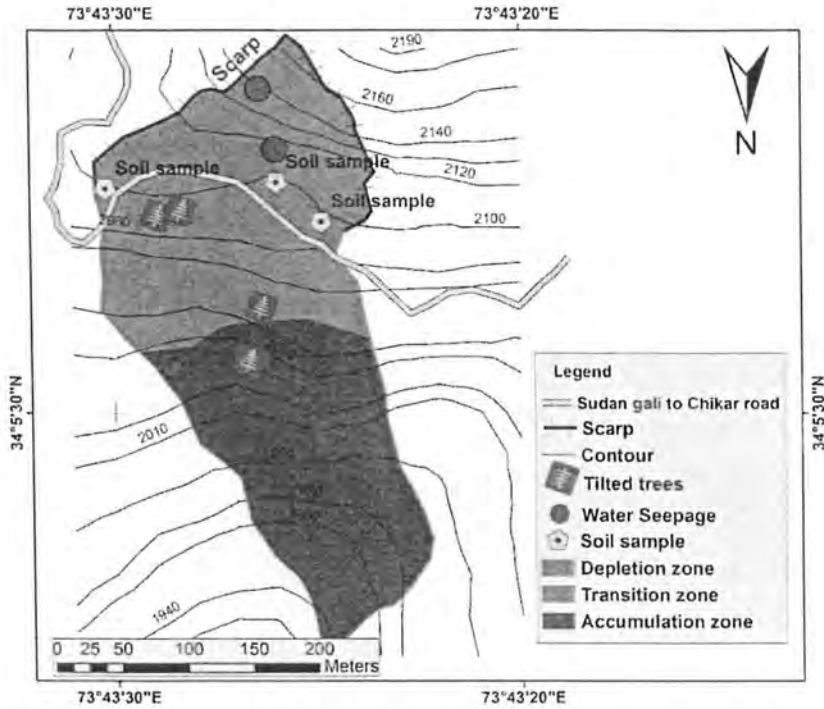


Fig.5.4 The three zones of the Sarbala landslide, the main scarp, and the water seepage are depicted on a map.

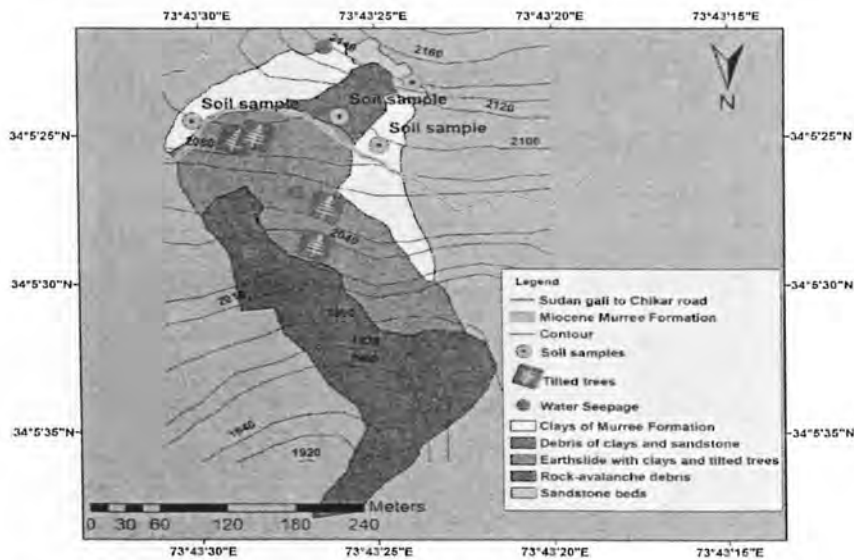


Fig.5.5 A geological map of the Sarbala landslide shows that the upper portion of the slide is composed of clays and sandstone from the Murree Formation, while the lowest portion is made up of debris and large sandstone boulders.

5.1.2.6 Types of movements in Sarbala landslide

The body of Sarbala Landslide is dominantly composed of sliding mass which is composed of detached soil mass, gravel, and boulders. According to the classification scheme of (Varnes, 1978) the Sarbala Landslide is classified as translational and rotational slide. The upper part of landslide is rotational earth slide shown in (Fig 5.6) and lower part of landslide is translational slide. Earth slide is observed in the upper part of the landslide which is formed due to the failure of loose soil upon interacting with water.

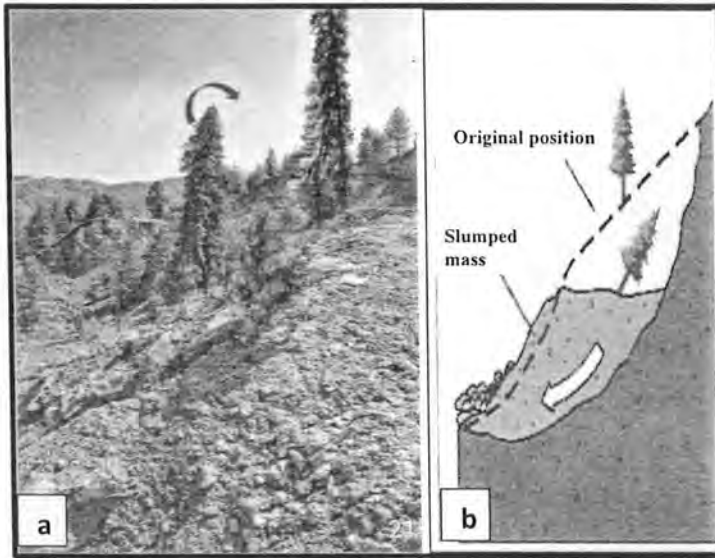


Fig. 5.6 **a** Downslope view of rotational earth slide documented in Sarbala landslide. **b** Schematic view of rotational slide (USGS Landslide Fact Sheet 2004-3072).

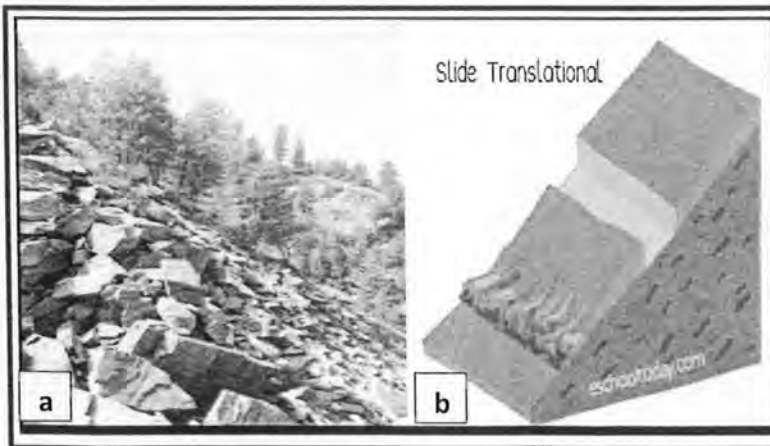


Fig.5.7 **a** Showing translational slide in Sarbala landslide. **b** Schematic view of translational slide (USGS Landslide Fact Sheet 2004-3072).

5.2 ERT Results:

The data was acquired using the Schlumberger configuration in the field. The data were processed by using the RES2D software to get 2D geoelectrical subsurface section based on ERT technique.

5.2.1 ERT-01 section

The profile ERT-01 was acquired from near the crown of Sarbala landslide using the Schlumberger configuration. Google earth imagery with ERT section is shown in (Fig 5.8).

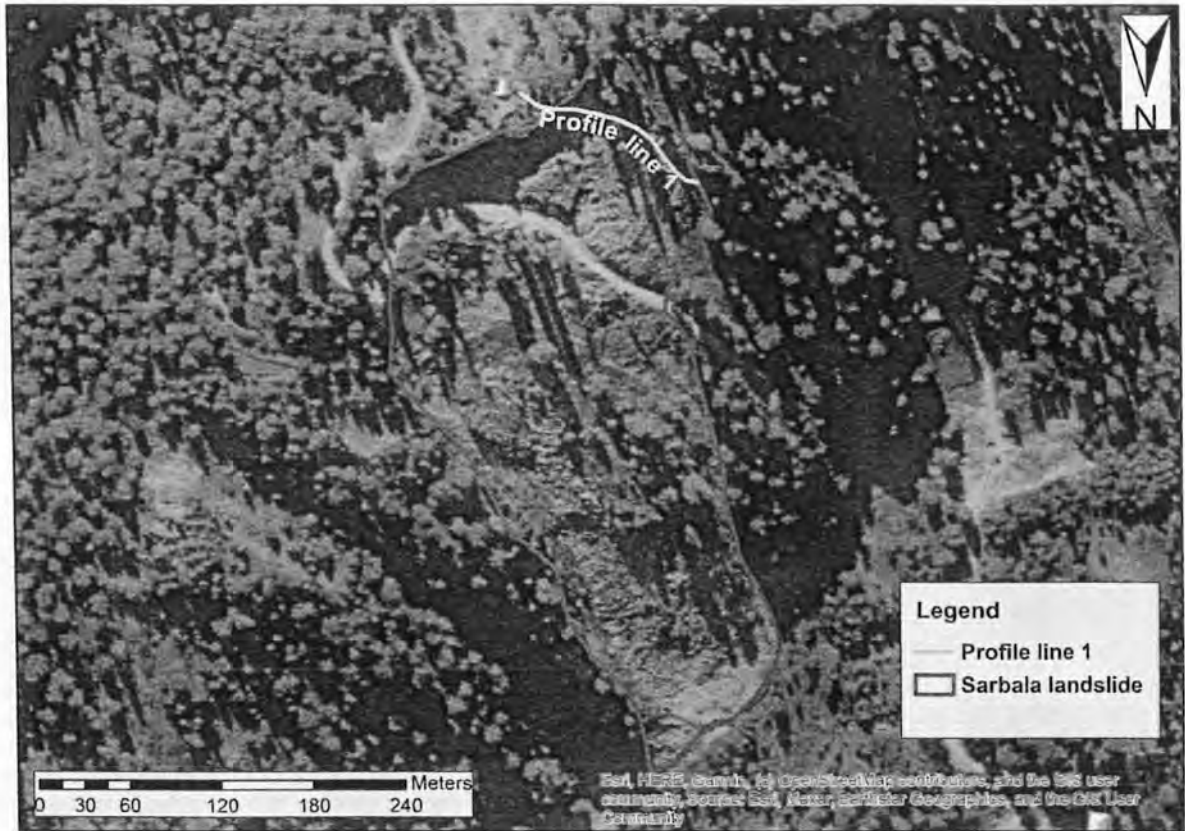


Fig.5.8 Google earth imagery showing ERT profile 1 taken from near the crown of Sarbala landslide.

The section based on the Schlumberger configuration delineated a High Resistivity Zone (HRZ) with resistivity values greater than 882-2907-ohm (Khaki, Red and purple color) indicated boulders, consolidated shales and dry sandstone. Maximum resistivity in this zone is 2907 Ωm which is interpreted as the bedrock of sandstone and mudstone of Murree Formation. The intermediate zone with a resistivity range (80-268 ohm) is indicated by green and yellow colors showing the saturated clays and mudstone of Murree Formation. The low resistivity zones (0-80 ohm) with blue color

indicate water seepages in clays (Fig 5.9). Low values of resistivity in this zone are due to the presence of saturated soil, colluvium, clays, and subsurface water channels.

The zone of low resistivity is interpreted as a sliding mass. Surface water infiltrates into the subsurface through fractures and fissures present in landslide mass and increases the moisture content of the sliding material consequently reducing the soil strength by adding unit weight. The overburden thickness is calculated along this profile is 25 m. and slip surface is lying at 25 m depth from the surface elevation 2090 m.

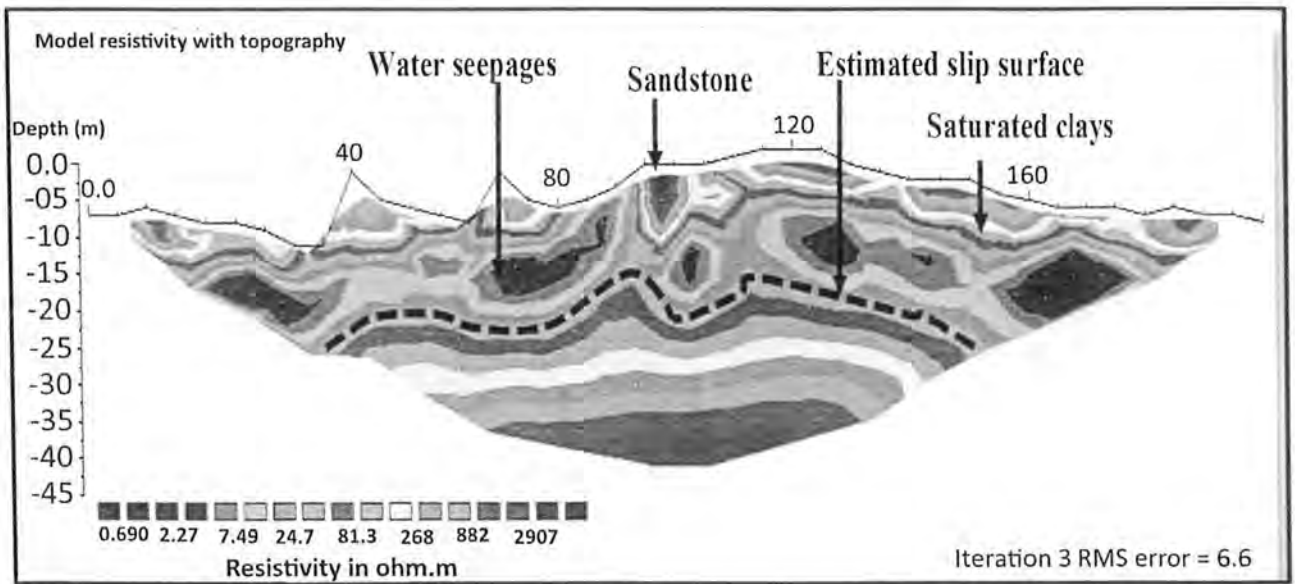


Fig. 5.9 Displays distribution of resistivity values in ERT section1 taken from near the crown of Sarbala landslide. Black dashed line shows the slip surface of landslide. Color rectangles show the resistivity values.

5.2.2 ERT-02 Section.

The profile ERT-02 was acquired along the road as shown in (Fig 5.10) using the Schlumberger configuration. The total horizontal distance covered in this profile is 200 m and the depth of investigation is 40 m (between 2065-2105). The data were processed by using the RES2D software to get 2D geoelectrical subsurface section based on ERT technique.

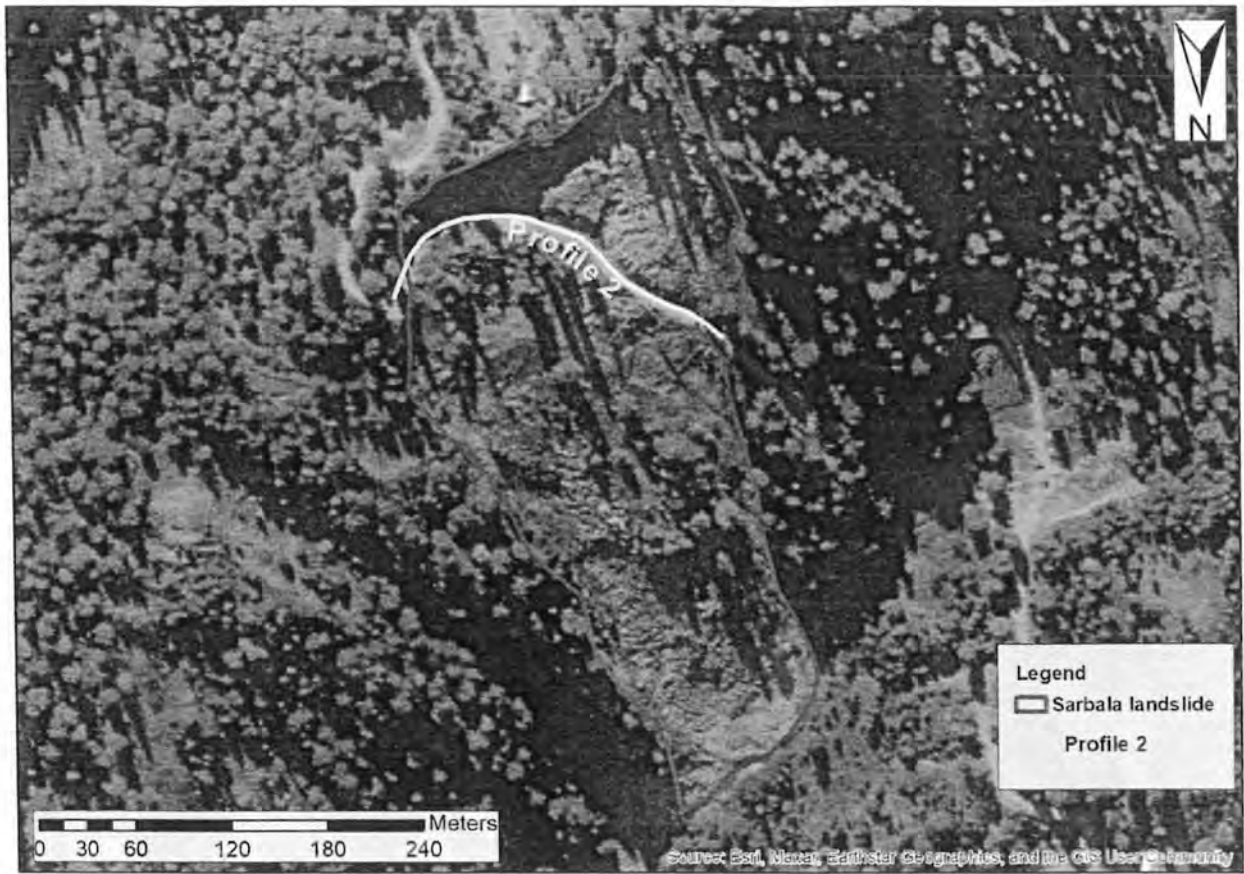


Fig.5.10 Google earth imagery showing ERT Profile 2. This ERT profile was collected from the road that was affected by the landslide in Sarbala.

ERT-02 section based on the Schlumberger configuration delineated a High Resistivity Zone (HRZ) with resistivity values greater than 543–3933-ohm (Khaki, Red and purple color) indicated boulders, consolidated shales, and dry sandstone. The intermediate zone with a resistivity range (70-543 ohm) is indicated by green and yellow colors showing the saturated clays and mudstone of Murree Formation. The low resistivity zones (0-70 ohm) with sky blue color indicate water seepages in clays. The zone of low resistivity represents the sliding mass which is comprised of saturated colluvium, clayey soil, and debris. Various surface water channels are also present along with this ERT profile which increases the water saturation of underlying mass (Fig 5.11). The overburden thickness is calculated along this profile is 35 m. and slip surface is lying at 35 m depth from the surface.

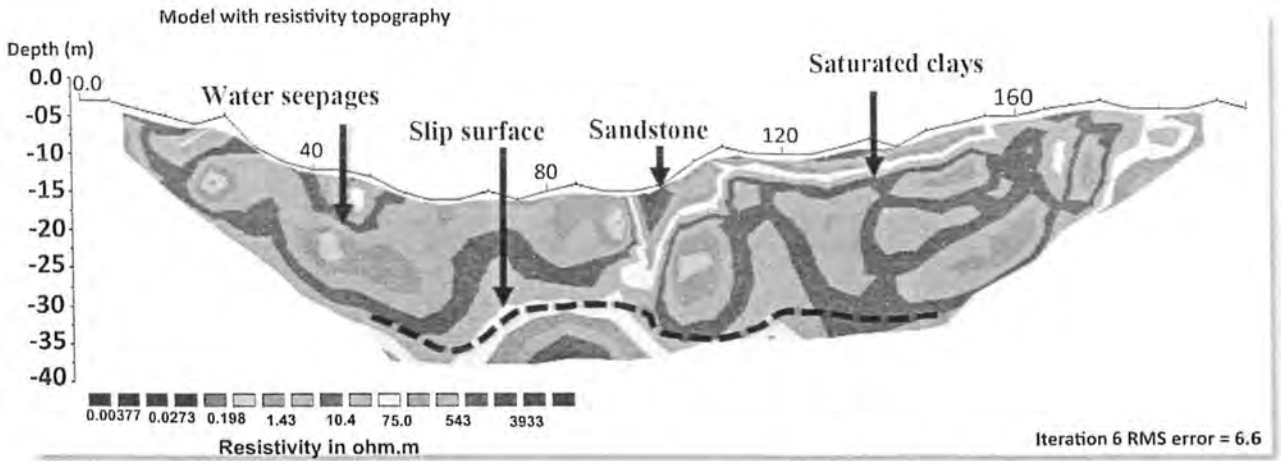


Fig. 5.11 Displays distribution of resistivity values in Profile 2. This ERT section was taken on Sudhan Gali to Chikar Road that is damaged by Sarbala landslide. Black dashed line shows the slip surface of landslide. Color rectangles show the resistivity values.

5.2.3 ERT-03 section

Below the road, the ERT-03 profile was acquired as shown in (Fig 5.12) using the Schlumberger configuration. The total horizontal distance covered in this profile is 200 m and the depth of investigation is 40 m (between 2075-2035).

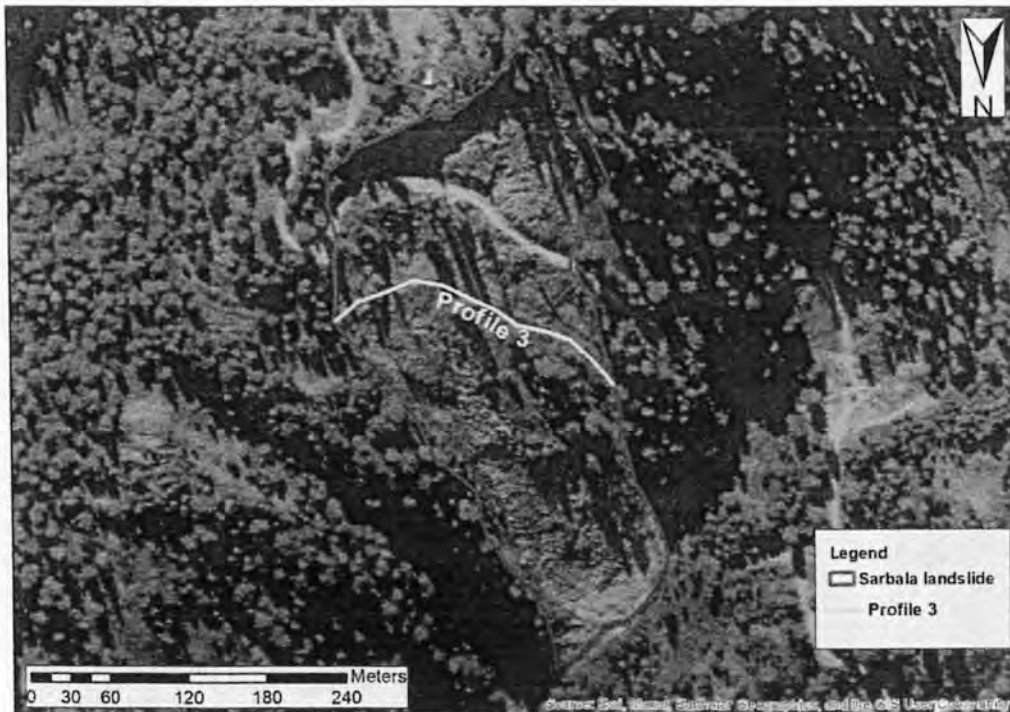


Fig. 5.12 Google earth imagery showing ERT profile 3. This ERT profile was taken from below the road.

The ERT-03 section based on the Schlumberger configuration delineated a High Resistivity Zone (HRZ) with resistivity values greater than 400–2359-ohm (Khaki and purple color) indicated boulders, and dry sandstone. This body of high resistivity value is interpreted as fractured Sandstone. The intermediate zone with a resistivity range (70-200 ohm) is indicated by green and yellow colors showing the saturated clays and mudstone of Murree Formation. The low resistivity zones (0-35 ohm) with blue color indicate water seepages in clays (Fig 5.13). The zone of low resistivity represents the sliding mass which is comprised of saturated colluviums and debris. Various surface water channels are also present along with this ERT profile which increases the water saturation of underlying mass. The overburden thickness is calculated along this profile is 40 m and slip surface has not been demarcated at this location up to depth of 40 m. The area of landslide showing accumulation of thick overburden.

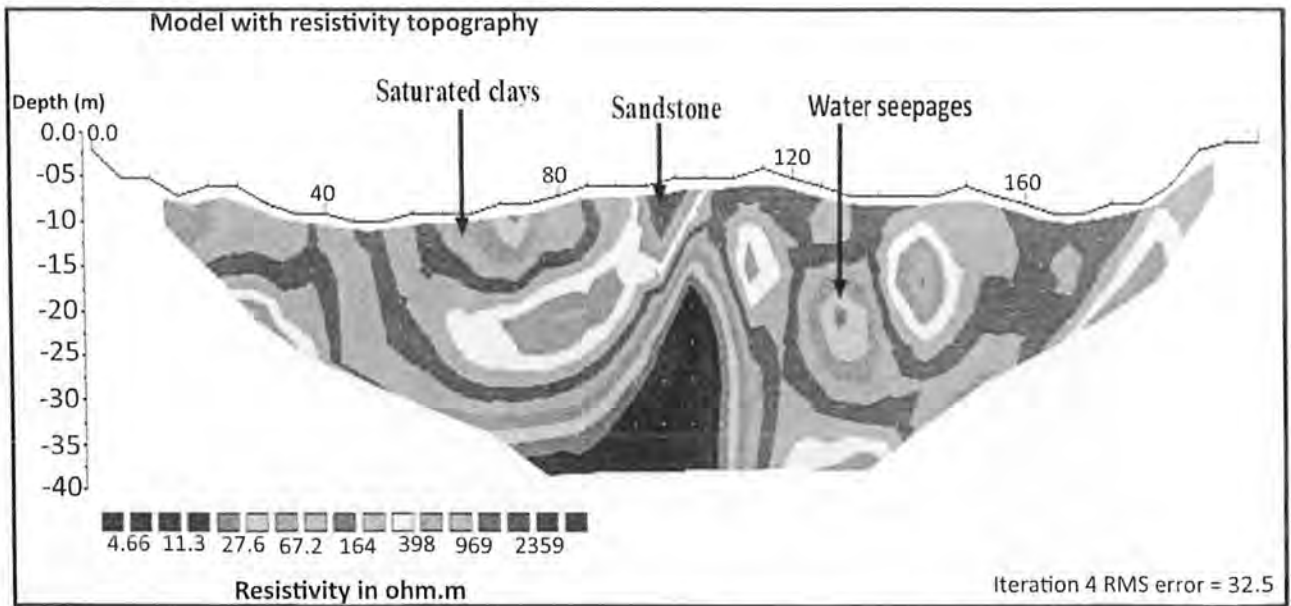


Fig. 5.13 Displays distribution of resistivity values in ERT 3 acquired from below the road. The resistivity values are represented by colored rectangles.

5.2.4 ERT-04 section

The profile ERT-04 was acquired from the center of landslide as shown in (Fig 5.14) using the Schlumberger configuration. The total horizontal distance covered in this profile is 200 m and the depth of investigation is 40 m (between 2015-2065). Resistivity values in this model section range from 0.115Ωm to 1178 Ωm.

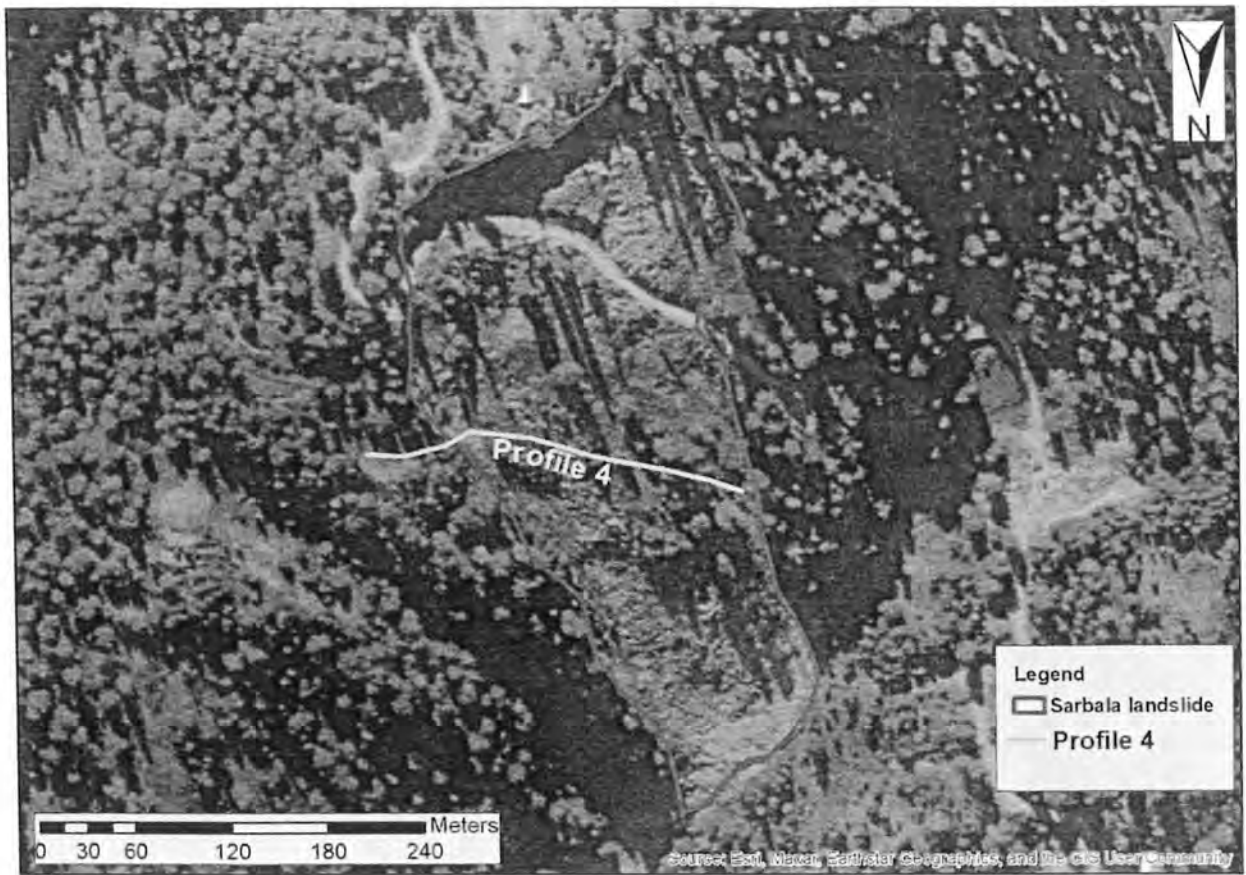


Fig. 5.14 Google earth imagery showing ERT Profile 4. This ERT profile was taken from the center of Sarbala landslide.

ERT-04 section based on the Schlumberger configuration delineated a High Resistivity Zone (HRZ) with resistivity values greater than 300–1178-ohm m (Khaki, red and purple color) indicated boulders, and dry sandstone. The third zone is the zone of high resistivity with resistivity values ranging from 300Ωm to 1178Ωm. This high resistivity zone is interpreted as a bed rock of sandstone that extends in depth. The intermediate zone with a resistivity range (6-90 ohm) is indicated by green and yellow colors showing the saturated clays and mudstone of Murree Formation. The low resistivity zones (0-5 ohm) with blue color indicate water channel/ seepages in clays (Fig 5.15). Low values of resistivity in this zone are due to the presence of saturated soil, colluvium, clays, and subsurface water channels.

This zone of low resistivity is interpreted as a sliding mass. Surface water infiltrates into the subsurface through fractures and fissures present in landslide mass and increases the moisture content of the sliding material consequently reducing the soil strength by adding unit weight. The overburden

thickness is calculated along this profile is 15 m and slip surface has been demarcated at this location up to depth of 15 m. The Toe area of landslide showing accumulation of less thick overburden.

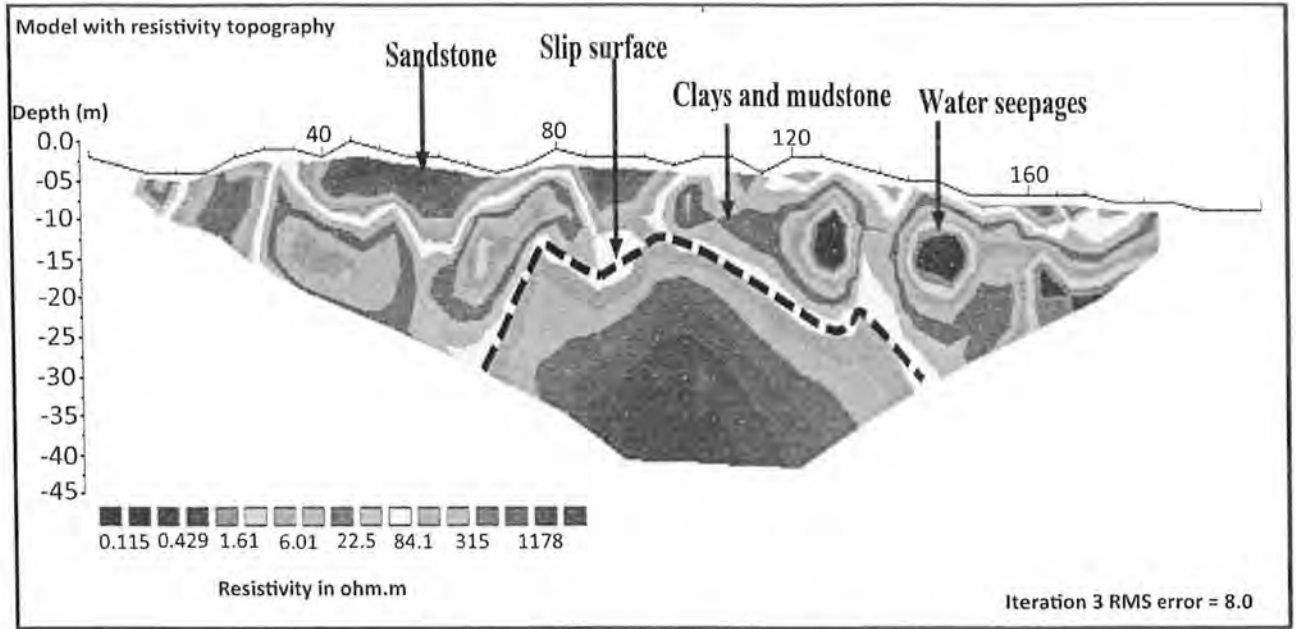


Fig. 5.15 Displays distribution of resistivity values in Profile 4 taken from the center of Sarbala landslide. Black dashed line shows the slip surface of landslide. Color rectangles show the resistivity values.

5.2.5 ERT-05 section

The profile ERT-05 was acquired from near the Toe of landslide as shown in (Fig 5.16) using the Schlumberger configuration. The total horizontal distance covered in this profile is 200 m and the depth of investigation is 45 m (between 2005-2050 m). This section displays the resistivity distribution in three distinct zones, which are the low, intermediate, and high resistivity zones. Resistivity values in this model section range from 0 Ω m to 1178 Ω m.

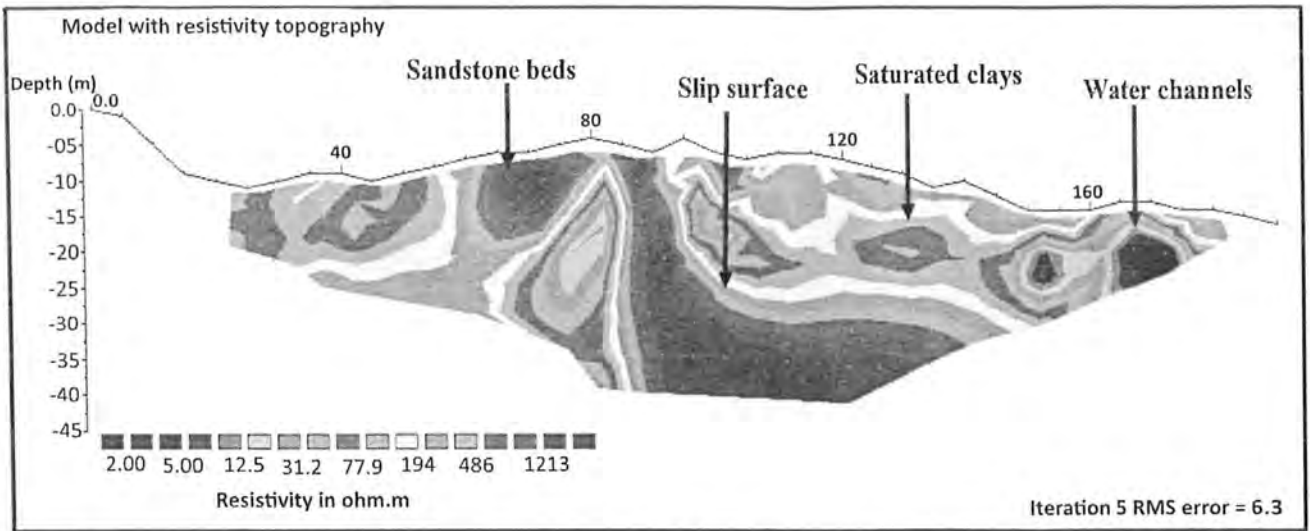


Fig. 5.17 Displays distribution of resistivity values in ERT 05 taken from near the toe of Sarbala landslide. Color rectangles show the resistivity values.

5.2.6 ERT-06 section

The profile ERT06 was acquired vertically from crown to toe using the Schlumberger configuration. This ERT profile was taken vertically from north to south of Sarbala landslide as shown in Google earth imagery integrated with ERT Profile 6 (Fig 5.18). The total horizontal distance covered in this profile is 200 m and the depth of investigation is 40 m (between 2140-2000 m).

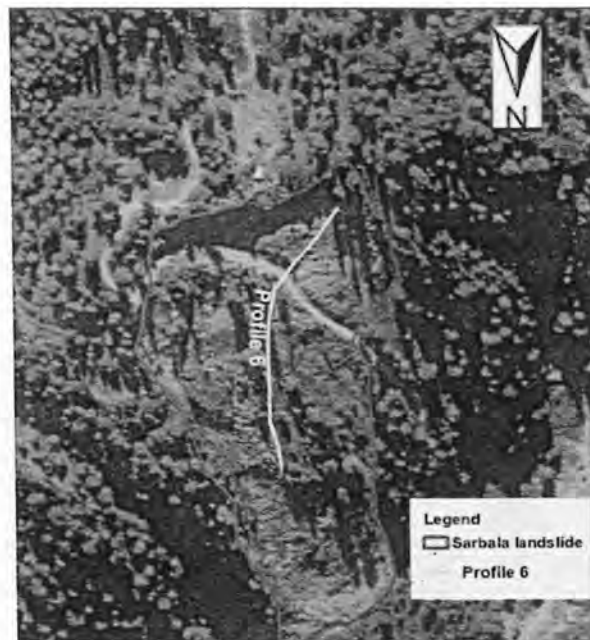


Fig. 5.18 Google earth imagery showing ERT Profile 6. This ERT profile was taken vertically from north to south of Sarbala landslide.

This section (Fig. 5.19) based on the Schlumberger configuration delineated a High Resistivity Zone (HRZ) with resistivity values greater than 250–2535-ohm (Khaki, red and purple color) indicated boulders, and dry sandstone. The intermediate zone with a resistivity range (19-250 ohm) is indicated by green and yellow colors showing the saturated clays and mudstone of Murree Formation. The low resistivity zones (0-19ohm) with blue color indicate water channel seepages in clays. One interpretation of this region of low resistivity is a moving mass. Through the fractures and fissures existing in the landslide mass, surface water seeps into the subsurface and raises the moisture content of the sliding material, hence decreasing the soil's strength by adding weight. The overburden thickness is calculated along this profile and is variable between 15 -35 m.

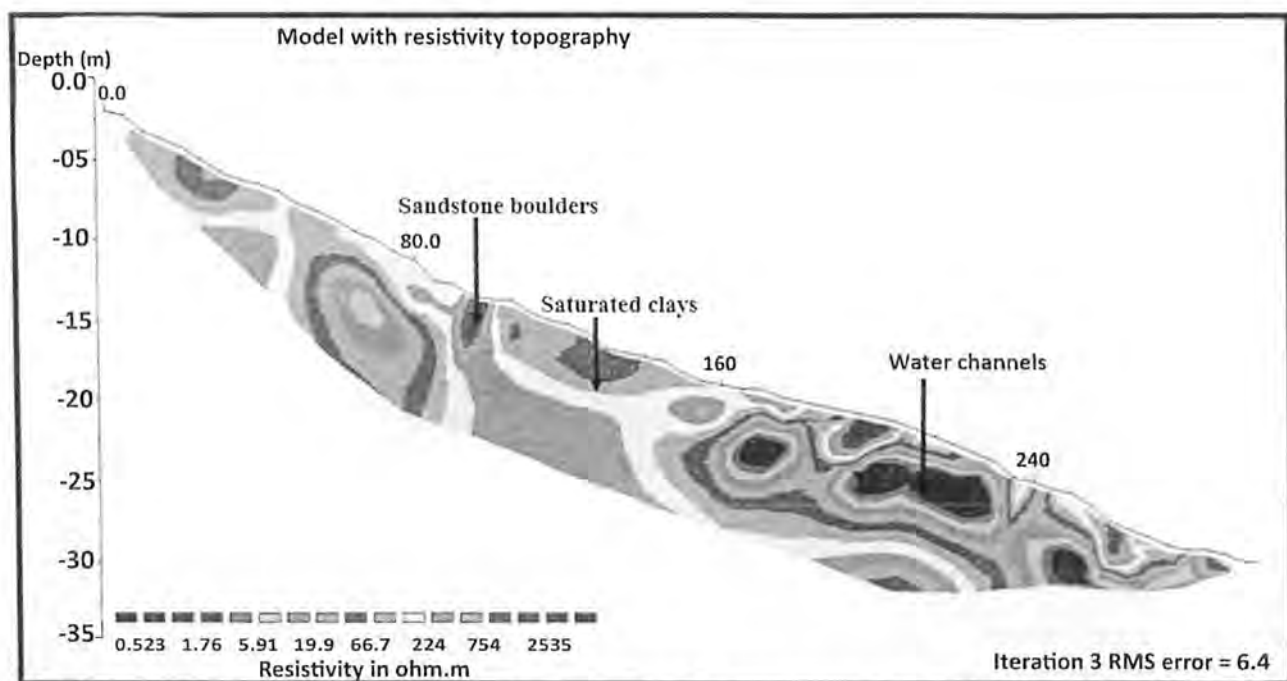


Fig. 5.19 Displays distribution of resistivity values in ERT section taken vertically from Sarbala landslide. Color rectangles show the resistivity values.

5.3 Electrical resistivity 3D models

The 3D view of ERT profiles in different directions show extension of different geological units horizontally and vertically. These profiles show bed rocks at crown and toe side, but central part of the landslide demarcated thick overburden and bedrock is not visible in this part up to 40 m depth. These Figures also depicted that water seepages are observed in continues pattern from crown to Toe (Fig 5.20, 5.21, 5.22).

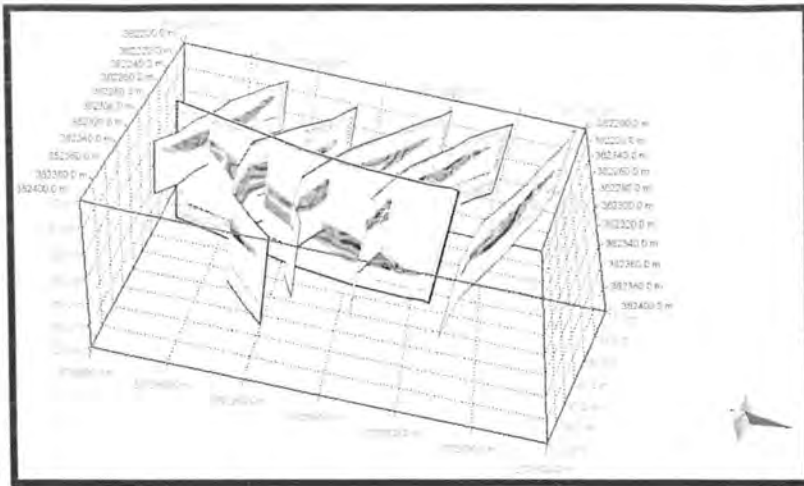


Fig. 5.20 3D view of ERT profiles showing different geological units and water seepages in a continuous pattern.

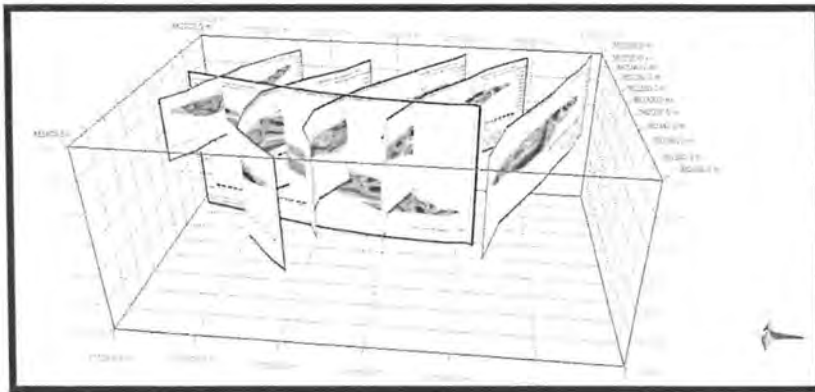


Fig. 5.21 3D view of ERT profiles showing different geological units and water seepages in a continuous pattern.

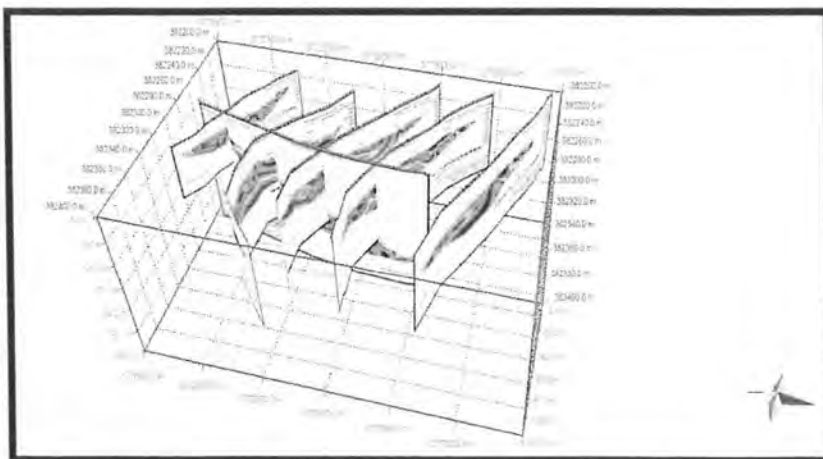


Fig. 5.22 3D view of ERT profiles in different directions.

5.4 Geotechnical Test

On soil samples from the Sarbala landslide, four different tests were performed to identify their physical and mechanical properties, which are as follows.

5.4.1 Sieve Analysis

Using a sieve analysis (or gradation test), you can measure the material's particle size distribution (the gradation) by passing the material through successively smaller mesh sizes and then weighing the amount that is stopped as a percentage of the total mass. Three samples were used to determine the percentage of materials that passed through sieves #0.75, #0.5, #0.375, #4, #40, #50, #100, and #200 are shown in Table 3.2.

Table 3.2 shows the percentage of samples passing from different sizes of the sieve.

Sieve Diameter (mm)	% Passing of Right flank soil sample	% Passing of Left flank soil sample	% Passing of Center of soil sample
19	100	100	100
12.50			
9.50	90.1443	96.2093	79.3674
4.70			
0.43	25.5269	40.5728	22.6197
0.30			
0.150	10.5757	11.2177	10.3012
0.075			

The graph shows the percentages of finer material passing through different sieves in (Fig5.23) grain diameter at the x-axis and %age of pass at the y-axis. It shows that the material is mostly sandy and gravel which is 50% and 45% approximately, fines is about 5%. In field investigation, we also observed that the material is mostly sandy, clay, and some boulders of sandstone of Murree formation are also observed.

Particle Size distribution curve Curve

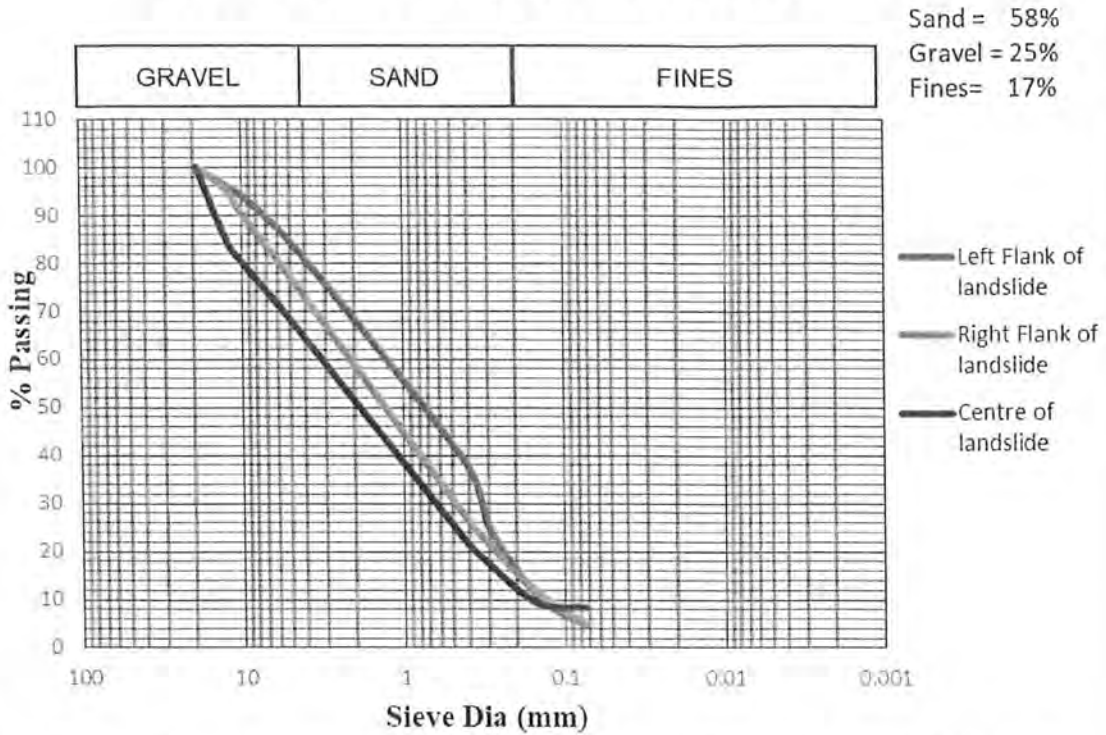


Fig. 5.23 showing particle distribution curve of samples collected from Sarbala landslide.

5.4.2 Specific Gravity

A soil's specific gravity is a measure of its quality or strength. Specific gravity is defined as the ratio of material to water.

The formula for Specific Gravity

$$\text{Specific Gravity} = \frac{(W_2 - W_1)}{(W_4 - W_1) - (W_3 - W_2)} \quad (6)$$

where, W1 is the weight of pycnometer (g), W2 is the weight of pycnometer and dry soil (g), W3 is the weight of pycnometer, soil with water and w4 is the weight of pycnometer and water. The values of specific gravity of all samples are shown in Table 3.3.

Results

The average specific gravity of samples collected from landslide is 2.35 shown in Table 3.2. The specific gravity values indicate that soil is mostly sand with minor silt and clays and have high porosity and permeability, therefore more water entered the subsurface, causing the soil to break down and resulting in slope failure.

Table 3.2 shows the percentage of samples passing from different sizes of the sieve.

Sample Number	Sample Name	Specific gravity
SLS 1	Right Flank of Landslide	2.225
SLS 2	Centre of Landslide	2.656
SLS 3	Left Flank of Landslide	2.19

5.4.3 Atterberg Limit

The Atterberg limits are a simple evaluation of a fine-grained soil's crucial water content: its plastic and liquid limitations. The variation in soil behavior may thus be used to identify the boundary between the two conditions. Soil Classification System by AASTHO is shown in (Fig 5.24).

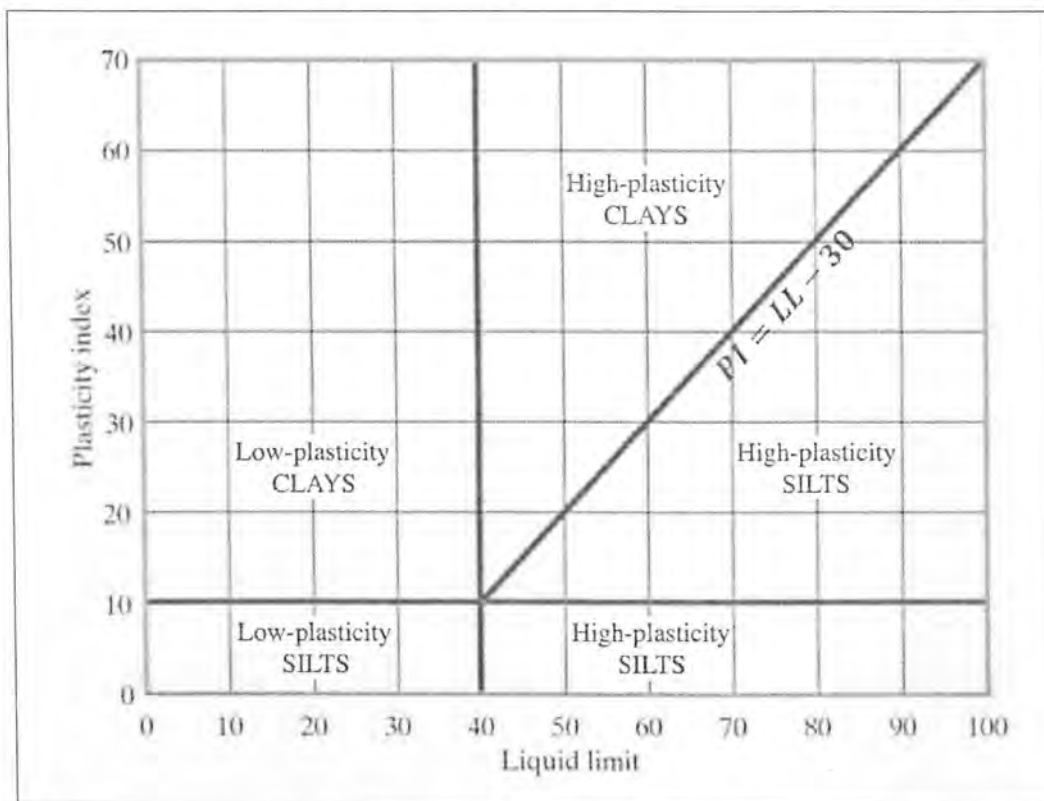


Fig.5.24 Soil Classification System by AASTHO (American Association of State Highway and Transportation Officials).

5.4.3.1 Liquid Limit of Right flank

The liquid limit of sample collected from right flank of landslide is shown in (Fig. 5.25). The graph is plotted between moisture content %age at y-axis and numbers of blows at x-axis. The Liquid limit is 27 and the Plastic limit is 17. The Plasticity index of the Right flank soil sample from Sarbala landslide is 10 which indicate that the soil possesses low plasticity which refer that cohesion between soil particles are low, therefore, when soil wet has least impact rather than liquefaction. In field investigation, small drainages were also found in that area.

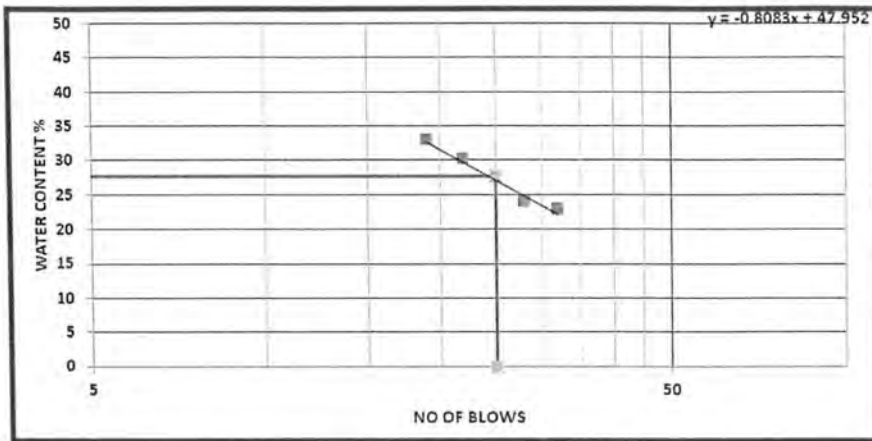


Fig. 5.25 Liquid limit of sample collected from the Right flank of Sarbala landslide.

5.4.3.2 Liquid Limit Centre of landslide

The liquid limit of sample collected from the Centre of landslide is shown in (Fig. 5.26). The graph is plotted between moisture content %age at y-axis and numbers of blows at x-axis. The Liquid limit is 21 and the Plastic limit is 14. The Plasticity index of soil sample from Centre of Sarbala landslide is 7 which indicates that the soil possesses low plasticity which refers to that cohesion between soil particles is low, therefore, the soil is sandy soil, low plastic, and partly cohesive.

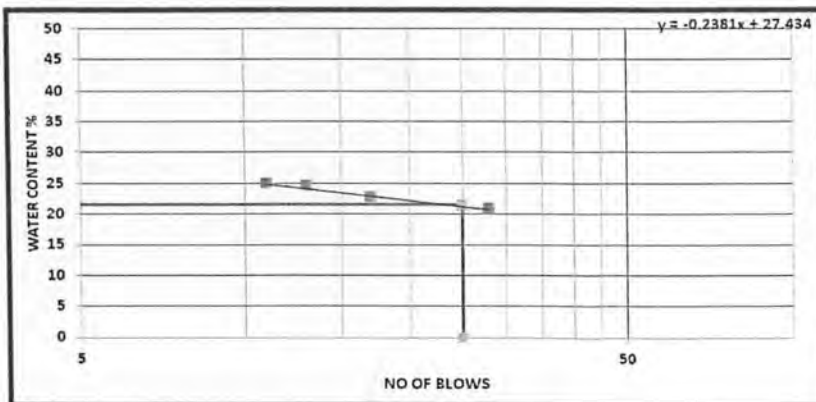


Fig. 5.26 Liquid limit of sample collected from the center of slide.

5.4.3.3 Liquid Limit of Left flank

The liquid limit of sample collected from left flank of landslide is shown in (Fig.5.27). The graph is plotted between moisture content %age at y-axis and numbers of blows at x-axis. The Liquid limit is 23 and the Plastic limit is 14. The Plasticity index of the left flank soil sample from Sarbala landslide is 9 which indicate that the soil possesses low plasticity which refer that cohesion between soil particles are low, therefore the soil is sandy soil, low plastic, and partly cohesive.

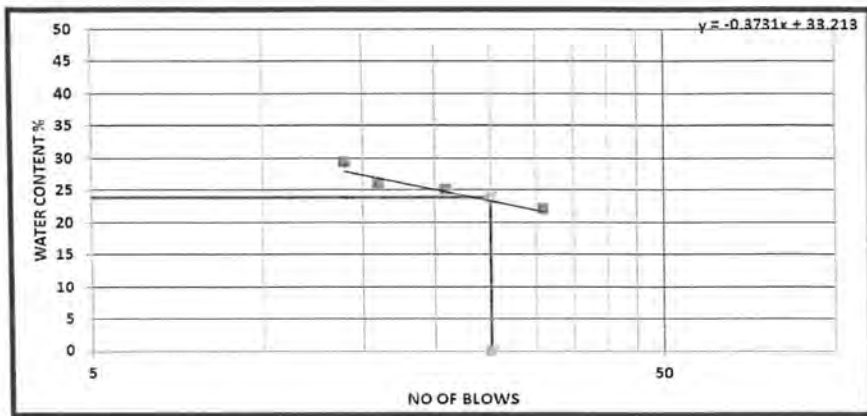


Fig. 5.27 Liquid limit of sample collected from the left flank of Sarbala landslide.

5.4.4.1 Proctor Compaction Test of right flank

To determine the compaction test was performed on a sample collected from the right flank of the landslide. The optimum moisture content (OMC) of right flank soil samples is 16.78% and maximum dry density (MDD) is 1.8 g/cc, respectively (Fig. 5.28). Maximum dry density and optimal moisture content values indicate that compaction effort may result in cracking, indicating non-cohesive soil.

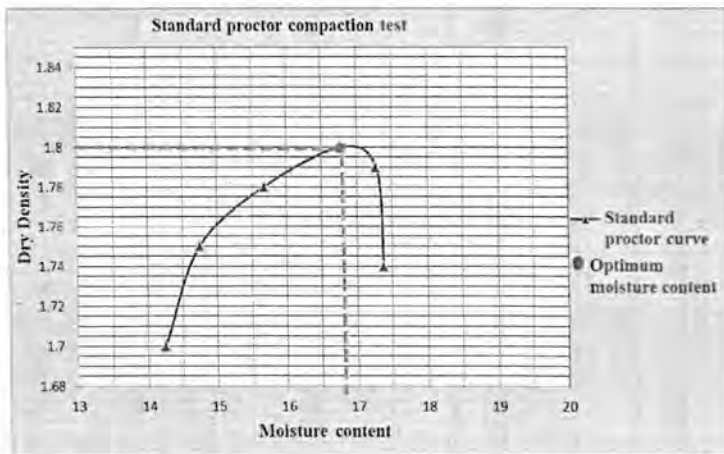


Fig. 5.28 Standard proctor compaction curve showing optimum moisture content and maximum dry density from the right flank of landslide.

5.4.4.2 Proctor Compaction Test of left flank

Compaction test was performed on sample collected from left flank of landslide. The proctor test was used to determine the maximum dry density and ideal moisture content of the soil sample taken from the landslide. This test was carried out to measure the OMC and Maximum Dry Density of the soil. The optimum moisture content (OMC) of left flank soil samples is 14.57 % and its maximum dry density (MDD) is 1.83 g/cc (Fig. 5.29). Maximum dry density and optimum moisture content values indicate that compaction effort may produce cracking which indicates non cohesive soil.

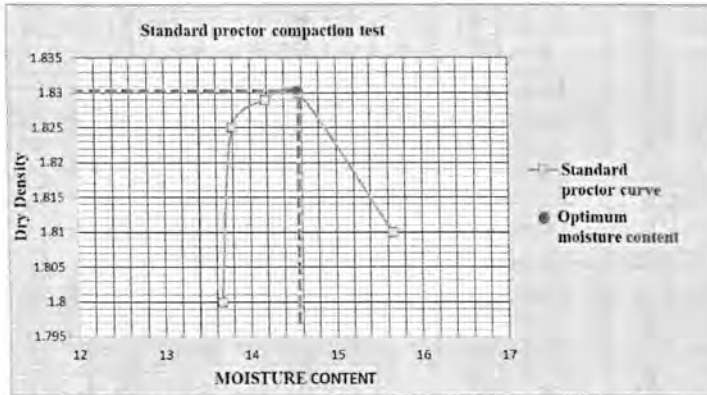


Fig. 5.29 Standard proctor compaction curve showing optimum moisture content and maximum dry density from left flank of landslide.

5.4.4.3 Proctor Compaction Test center of landslide

To work out the compaction test was performed on collected sample from center of landslide. This test was carried out to measure the OMC and MDD of the soil. The optimum moisture content (OMC) of soil samples from center of landslide is 13.78 % and its maximum dry density (MDD) is 1.9 g/ccm (Fig. 5.30). Maximum dry density and optimum moisture content values indicate that compaction effort may produce cracking which indicates non cohesive soil.

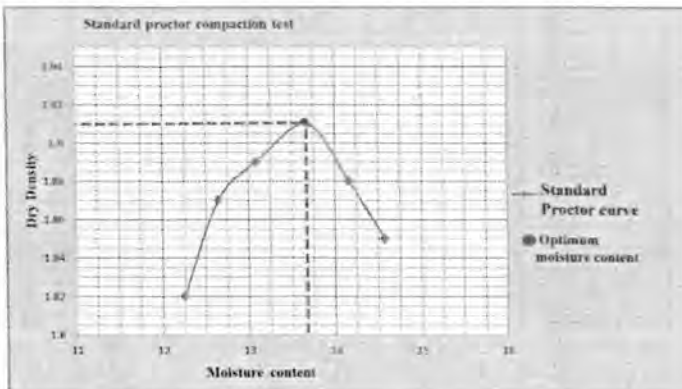


Fig. 5.30 Standard proctor compaction curve showing optimum moisture content and maximum dry density from center of landslide.

DISCUSSION AND CONCLUSIONS

6.1 Discussion

The key aim of this study is to investigate the surface and subsurface dynamics of the Sarbala landslide by use of geophysical and engineering techniques. 2D ERT and Geotechnical laboratory tests for properties soil were executed on landslide samples have been applied to extract the surface and subsurface characteristics of the Sarbala Landslide. The studied landslide is initiated in the Miocene Murree Formation due to heavy rain falls in April 2018. Surface characteristics including multiple failure mechanisms of landslide depict the two types of slides nature of landslide i.e., rotational, and translational slide. Multiple tensional cracks present along the slope and at the crown indicating the active nature of landslide. The Electrical Resistivity Tomography (ERT) method is widely used to understand the geometry and failure mechanism of landslides (Perrone et al., 2014). The ERT survey was carried out by Batayneh and Al-Diabatin (2002) to investigate a landslide along the Amman-Dead Sea highway in Jordan. The results showed that shales and limestones were present in the subsurface. 2D ERT results indicate the control of hydrogeology on instability of Sarbala landslide. A well-developed Slip surface is observed between unconsolidated landslide mass and underlying bedrock based upon resistivity contrast. Resistivity values in six ERT Profiles taken in Sarbala landslide range between $10.9 \Omega\text{m}$ to 3933Ω with lowest values indicating water saturated colluvium comprising landslide mass and higher resistivity values indicating bedrock and gravels. The field investigation revealed that the Sarbala landslide is predominantly consists of clays and sandstone of Murree Formation. In laboratory studies of landslide material, the gradation test revealed that most of the soil was sandy, and that different proportions of silt and clay were present.

Atterberg properties, which have a strong influence on mass movement, are soil texture, porosity and permeability, soil mineral content, and soil water content (Heshmati et al. 2011). The plastic limit separates the soil's plastic and semisolid states, whereas the liquid limit separates the soil's plastic and flow states (Campbell, 2001). The Atterberg limits of the landslide material indicated plasticity index of the soil samples from Sarbala landslide range 7- 10 which indicate that the soil possesses low plasticity which refer that cohesion between soil particles are low, therefore the soil is sandy soil, low plastic, and partly cohesive. Xu (1996) found that the shear strength between the soils particles rapidly decreases due to an increase in pore pressure caused by an increase in water content. The specific gravity values of Sarbala landslide samples indicates that soil is mostly sand with minor silt and clays

and have high porosity and permeability, therefore more water entered the subsurface, causing the soil to break down and resulting in slope failure. Zhang et al. (2012) demonstrated that variations in soil moisture content can modify the pore pressure, swelling and increase the self-weight of the soil, hence changing the shear strength, and stability which affects the process of gravitational erosion. High water content causes fractures that weaken the soil's capacity and ultimately lead to its collapse. Moreover, the MDD and OMC values indicate that compaction effort may produce cracking which indicates low cohesive soil.

Tectonically this area is active and bounded by two active faults i.e., are Bagh Balakot fault and Jhelum fault. The landslide analysis with respect to fault distance reveals that Sarbala landslide is located within 5km buffer of Bagh Balakot fault and Jhelum fault is located within 10 km diameter from Sarbala landslide are shown (Fig.5.31). Distance to fault map reveals that these two faults are located within the diameter of 3-10 km from Sarbala landslide and play key role for the triggering of landslide. These two faults are major causative factors for the Sarbala landslide and many other landslides in this area. This study suggests the implication of more advanced research for monitoring of Sarbala landslide in future.

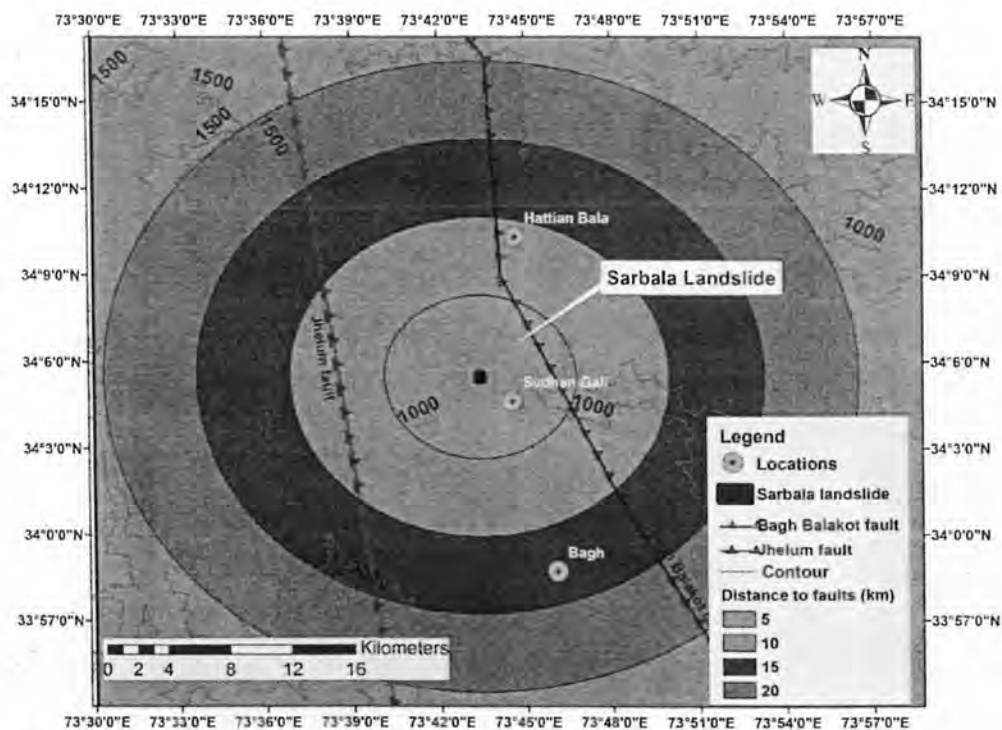


Fig.5.31 Map showing landslide distance to Jhelum fault and Bagh Balakot fault in the study area.

Earthquakes contribute significantly to the landslide hazards. Strong slopes fail because of the strains created by earthquakes, and landslides have been observed to occur after earthquakes of a magnitude of 4.0 and higher. The M-7.6 Kashmir earthquake of October 8, 2005 generated thousands of landslides in Kashmir. Basharat et al., (2012) studied the Hattian Bala rock landslide which is the biggest landslide caused by 2005 Kashmir earthquake. This slope movement blocked two major streams of the area which are tributaries of the river Jhelum is the largest landslide caused by the earthquake occurred in the Miocene Murree Formation, which consist of sandstone, mudstone, shale, and limestone, this landslide is a debris avalanche with a volume of about 80 million cubic meters. According to locals, the avalanche killed almost 1,000 people, buried the village of Dandbeh, and destroyed the town. Movement at Sarbala starts after October 8, Kashmir earthquake as shown in historical image of google earth (Fig. 5.32).



Fig.5.32 Historical image after 2005 Kashmir earthquake showing movement at study area before the landslide occurs.

6.2 Conclusions

- Sarbala landslide has slide nature of movement with both rotational and translational slide movement and is active in the present form as inferred from geomorphological features of landslide.
- Inverted electricity tomograms show that resistivity values of subsurface materials i.e., landslide mass and bedrock ranges from 0.0037 Ωm to 3933 Ωm . Low resistivity is caused by unconsolidated landslide material and water-saturated colluvium whereas high resistivity is caused by bedrock such as sandstone and mudstone of Miocene Murree Formation. The depth of landslide slip surface of Sarbala landslide ranges from 15 to 35 meters.
- It is sandy soil with gravel and clays and has low plasticity which refers to that cohesion between soil particles is low, as indicated by soil testing in the geotechnical lab. The specific gravity values of Sarbala landslide samples indicates that soil is mostly sand with minor silt and clays and have high porosity and permeability, which enables more water to infiltrate the strata and decrease pore water pressure, weakening the slope and finally dropping.
- Tectonically this area is active, Bagh Balakot fault and Jhelum fault play important role for triggering Sarbala landslide.
- Besides the geological nature of the area, geomorphological features i.e., steep slope angle, high topographic relief and drainage are major factors that are contributing to activation of Sarbala landslide.
- The probability of major reactivation of Sarbala landslide in future cannot be ruled out, this reactivation will cause extensive slope failure leading to the devastation of infrastructure present on the crown and near to the toe of landslide particularly the houses and Road.

6.3 Recommendations

Based on present research, the following recommendations are made for landslide mitigation to reduce the risks of damage caused by Sarbala landslide.

6.3.1 Administrative Measures

The areas which are at greater risk of landslide hazard should be evacuated and the community may be relocated by proper land-use planning. Construction of new buildings at the crown of Sarbala Landslide should be avoided as they can contribute to slope failure by adding the effect of gravity. Proper drainage planning should be done to avoid the infiltration of the soil mass by surface runoff.

6.3.2 Engineering Measures

To reduce the effect of driving forces and to increase the resisting forces of landslides some remedial measures are vital. Hydrogeological measures are important to consider for the prevention of addition in water saturation of slope mass. In the case of the Sarbala landslide, surface water should be diverted by the installation of pipes and ditches. Furthermore, to avoid infiltration by surface runoff, springs, and sewerage through cracks a single concrete water channel should be constructed. This channel may collect the water from the above discussed sources and drain out the water into nearby streams. Sealing of tensional cracks may be done using impervious materials such as bentonite clay. This may reduce the water infiltration through cracks. The slope geometry of Sarbala landslide may be modified to reduce the slope angles where steep slopes are present. This may be done by trenching or filling material at the toe of steep slopes. Slope reinforcement techniques i.e., installation of micro piles and construction of retaining structures can help to enhance the stability of landslides.

7 References

- Baig, M. S., & Lawrence, R. D. (1987). Precambrian to Early Paleozoic orogenesis in the Himalaya. *Kashmir Journal of Geology*, 5, 1-22.
- Baig, M., & Snee, L. (1995). The evidence for Cambro-Ordovician orogeny in northwest Himalayas Pakistan. *GeolSoci Am Abstr Program*, 27, 305.
- Baig, M. S., Yeats, R. S., Pervez, S., Jadoon, I. A., Khan, M. R., Siddiqui, I., Lisa, M., Saleem, M., Masood, B., & Sohail, A. (2010). Active tectonics, October 8, 2005, earthquake deformation, active uplifts, topography and seismic geohazards micro zonation, Hazara-Kashmir Syntaxis, North west Himalayas, Pakistan. *Journal of Himalayan Earth Sciences*, 43, 17-21.
- Basharat, M., Rohn, J., Baig, M. S., Khan, M. R., & Schleier, M. (2014). Large scale mass movement triggered by the Kashmir earthquake 2005, Pakistan. *Journal of Mountain Science*, 11(1), 19-30.
- Basharat, 2012. The distribution, characteristics and behavior of landslide triggered by the Kashmir Earthquake 2005, NW Himalaya, Pakistan, PhD thesis, University of Erlangen-Nuremberg, Germany, 186.
- Batayneh, A. T., & Al-Diabat, A. A. (2002). Application of a two-dimensional electrical tomography technique for investigating landslides along the Amman–Dead Sea highway, Jordan. *Environmental Geology*, 42(4), 399-403.

- Bossart, P., Dietrich, D., Greco, A., Ottiger, R., & Ramsay, J. G. (1988). The tectonic structure of the Hazara-Kashmir syntaxis, southern Himalayas, Pakistan. *Tectonics*, 7(2), 273-297.
- Brunsdon, D. (1993). Mass movement; the research frontier and beyond: geomorphological approach. *Geomorphology*, 7(1-3), 85-128.
- Barker, R. (1979). Signal contribution sections and their use in resistivity studies. *Geophysical Journal International*, 59(1), 123-129.
- Calkins, j. a., tw, o., &skm, a. (1975). geology of the southern Himalaya in Hazara, Pakistan and adjacent areas.
- Cheema, M. (1977). Cainozoic. Stratigraphy of Pakistan. *Memoirs of the Geological Survey of Pakistan*, Quetta, 12, 1-138, Cloud Compare. (2015). Cloud Compare version 2.6. 1 user manual.
- Coward, M. P., Butler, R. W. H., Chambers, A. F., Graham, R. H., Izatt, C. N., Khan, M. A., ... &Williams, M. P. (1988). Folding and imbrication of the Indian crust during Himalayan collision. *Philosophical Transactions of the Royal Society of London. Series A, Mathematical and Physical Sciences*, 326(1589), 89-116.
- Cruden, D. M., & Varnes, D. J. (1996). Landslides: investigation and mitigation. Chapter 3- Landslide types and processes. *Transportation research board special report (247)*.
- Campbell D.J.: Liquid and plastic limits. In: *Soil and environmental analysis-physical methods* (eds K.A. Smith & C.E. Mullins). Dekker Inc., New York. pp. 349-375, 2001.

Gansser, A. (1964). *Geology of the Himalayas*.

Gansser, A. (1981). The geodynamic history of the Himalaya. *Zagros Hindu Kush Himalaya Geodynamic Evolution*, 3, 111-121.

Greco, A. M. (1989). *Tectonics and metamorphism in the western Himalayan syntaxis area (Azad Kashmir, NE-Pakistan)* ETH Zurich.

Hemmat A, Aghilinategh N, Rezainejad Y, Sadeghi M (2010) Long-term impacts of municipal solid waste compost, sewage sludge and farm yard manure application on organic carbon, bulk density, and consistency limits of a calcareous soil in central Iran. *Soil Till Res* 108:43.

Heshmati M, Arifn A, Shamsuddin J, Majid NM, Ghaituri M (2011) Factors affecting landslides occurrence in agro-ecological zones in the merek catchment. *Iran J Arid Environ* 75:1072–1082.

Highland, L., & Bobrowsky, P. T. (2008). *The landslide handbook: a guide to understanding landslides*. US Geological Survey Reston.

Hungr, O., Evans, S., & Hutchinson, I. (2001). A Review of the Classification of Landslides the Flow Type. *Environmental & Engineering Geoscience*, 7(3), 221-238.

Hutchinson, J. N. (1988). Morphological and geotechnical parameters of landslides in relation geology and hydrogeology. In *Proc., Fifth international symposium on landslides, 1988*. Lausanne, AA.

- Jongmans, D., & Garambois, S. (2007). Geophysical investigation of landslides: a review. *Bulletin de la Société géologique de France*, 178(2), 101-112.
- Kamp, U., Growley, B. J., Khattak, G. A., & Owen, L. A. (2008). GIS-based landslide susceptibility mapping for the 2005 Kashmir earthquake region. *Geomorphology*, 101(4), 631-642.
- Kazmi, A. H., & Abbasi, I. A. (2008). *Stratigraphy & historical geology of Pakistan*. Department & National Centre of Excellence in Geology Peshawar, Pakistan.
- Kazmi, A. H., & Jan, M. Q. (1997). *Geology and tectonics of Pakistan*. Graphic publishers.
- Khan, M., Ali, M. (1994). Preliminary modeling of the western Himalaya. *Kashmir Journal of Geology*, 11(12), 59-66.
- Khan, A. N. Atta-ur-Rahman (2006) Landslide hazards in the mountainous region of Pakistan. *Pak J Geogr*, 16, 38-51.
- Koefoed, O. (1979). Resistivity sounding on an earth model containing transition layers with linear change of resistivity with depth. *Geophysical Prospecting*, 27(4), 862-868.
- Kristyanto, T. H. W., Indra, T. L., Syahputra, R., & Tempessy, A. S. (2017, May). Determination of the landslide slip surface using electrical resistivity tomography (ERT) technique. In *Workshop on World Landslide Forum* (pp. 53-60). Springer, Cham.

- Kitutu MG, Muwanga A, Poesen J, Deckers JA (2009) Influence of soil properties on landslide occurrences in bududa district, Eastern Uganda African. J Agric Res 4:611– 620.
- Loke, M. (1999a). Electrical imaging surveys for environmental and engineering studies. A practical guide to, 2. Loke, M. (1999b). Electrical imaging surveys for environmental and engineering studies. A practical guide to, 2,70.
- Merritt, A. J., Chambers, J. E., Murphy, W., Wilkinson, P. B., West, L. J., Gunn, D. A., ... & Dixon, N. (2014). 3D ground model development for an active landslide in Lias mudrocks using geophysical, remote sensing and geotechnical methods. *Landslides*, 11(4), 537-550.
- Mughal, M. S., Zhang, C., Du, D., Zhang, L., Mustafa, S., Hameed, F., Khan, M. R., Zaheer, M., & Blaise, D. (2018). Petrography and provenance of the Early Miocene Murree Formation, Himalayan Foreland Basin, Muzaffarabad, Pakistan. *Journal of Asian Earth Sciences*, 162, 25-40.
- Munir-ul-Hassan, m., Baig, m. s., & Mirza, k. upper cretaceous of Hazara and Paleogene biostratigraphy of Azad Kashmir, northwest Himalayas, Pakistan
- Perrone, A., Lapenna, V., & Piscitelli, S. (2014). Electrical resistivity tomography technique for landslide investigation: a review. *Earth-Science Reviews*, 135, 65-82.
- Pinfold, E. (1918). Notes on structure and stratigraphy in the North-West Punjab. *Rec. Geol. SurvIndia*, 49(3), 137-160.

- Palacky, G. J. (1988). Resistivity characteristics of geologic targets. *Electromagnetic methods in applied geophysics*, 1, 53-129.
- Rieux, K., Qureshi, R. A., Peduzzi, P., Jaboyedoff, M. J., Breguet, A., Dubois, J., Jaubert, R., Cheema, M. A., 2007. An interdisciplinary approach to understanding landslides and risk management: a case study from earthquake-affected Kashmir. *Mountain Forum, Mountain GIS e- Conference*, January 14-25, 2008.
- Sato, H. P., Hasegawa, H., Fujiwara, S., Tobita, M., Koarai, M., Une, H., & Iwahashi, J. (2007). Interpretation of landslide distribution triggered by the 2005 Northern Pakistan earthquake using SPOT 5 imagery. *Landslides*, 4(2), 113-122.
- Todd, D. K., & Mays, L. W. (2004). *Ground water hydrology*. John Wiley & Sons.
- Turab, S. A. (2012). *Structural geology of the surrounding of Muzaffarabad with emphasis of Neotectonics (Doctoral dissertation, M. Phil. Thesis, National Centre of Excellence in Geology, University of Peshawar)*.
- USGS Landslide Fact Sheet 2004- 3072
- Varnes, D. J. (1978). Slope movement types and processes. *Special report*, 176, 11-33.
- Wadia, D. (1931). The syntaxis of the northwest Himalaya: its rocks, tectonics, and orogeny. *Rec. Geol. Surv. India*, 65(2), 189-220.
- Wadia, D. N. (1928). The geology of Poonch State (Kashmir) and adjacent portions of the Punjab. *Mem. Geol. Surv. India*, 51, 185-370.

Wynne, A. (1874). Notes on the geology of neighbourhood of Mari hill station in the Punjab. India
Geol Survey Mem Rec, 7(2), 64-74. 98

Xu J. X.: Benggang erosion: the influencing factors, *Catena*, 27, 249-263, 1996.

Zohdy, A. A., Eaton, G. P., & Mabey, D. R. (1974). Application of surface geophysics to ground water investigations.